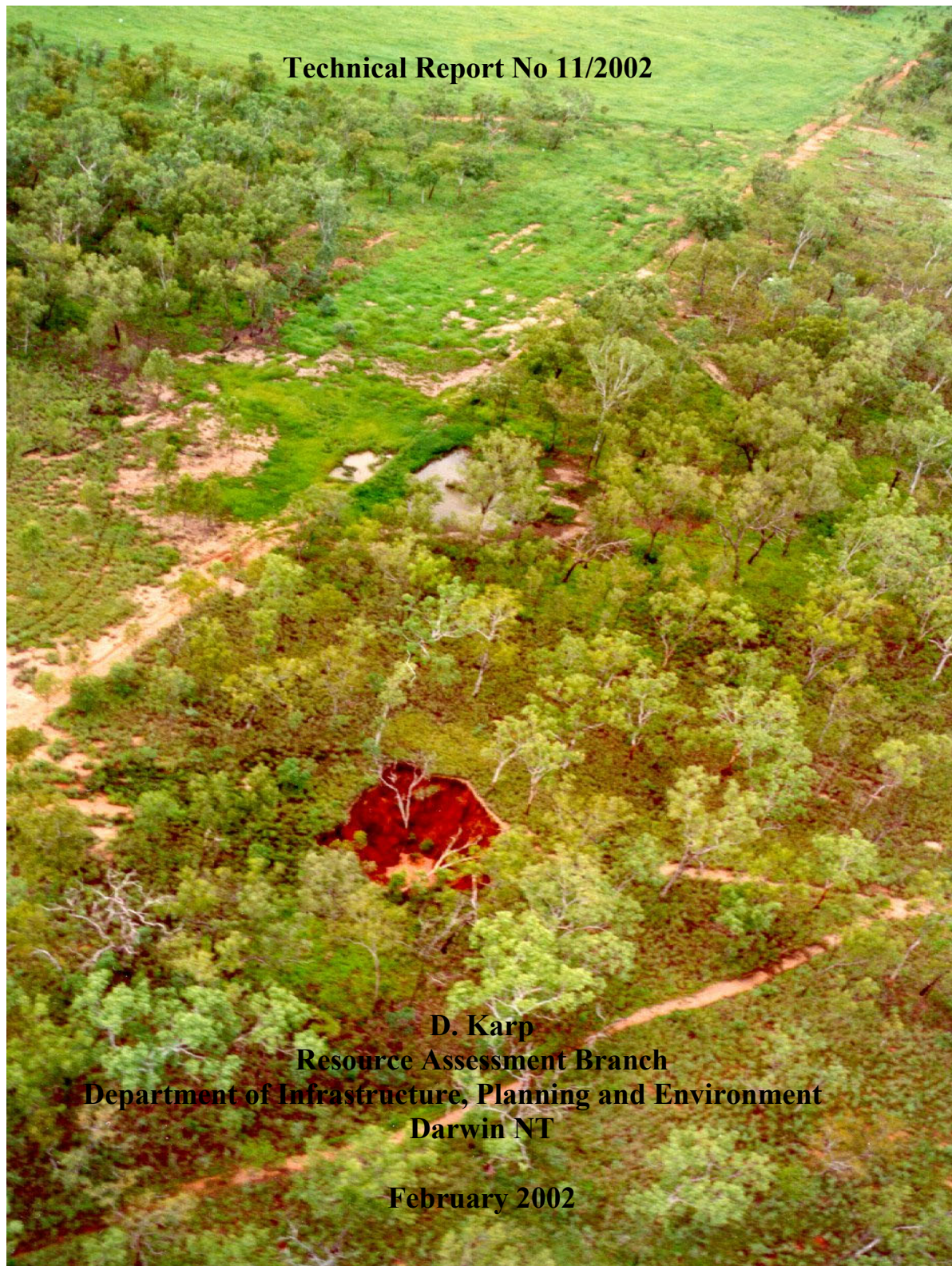


# LAND DEGRADATION ASSOCIATED WITH SINKHOLE DEVELOPMENT IN THE KATHERINE REGION

Technical Report No 11/2002



**D. Karp**  
**Resource Assessment Branch**  
**Department of Infrastructure, Planning and Environment**  
**Darwin NT**

**February 2002**



# **LAND DEGRADATION ASSOCIATED WITH SINKHOLE DEVELOPMENT IN THE KATHERINE REGION**

**D. Karp**

Resource Assessment Branch  
Department of Infrastructure, Planning and Environment  
Darwin NT

**February 2002**

Technical Report No 11/2002

Technical Report No. 11/2002

ISBN 0 7245 4823 8

The report is available from the Parks and Wildlife Commission of the Northern Territory (PWCNT) Library, the AZRI Library in Alice Springs and the National Library, Canberra, through interlibrary loan.

The report, both as a hard copy and in digital form (as a pdf), may be obtained from the Darwin Office of the Department of Infrastructure, Planning and Environment. Inquiries should be addressed to:

Director Resource Assessment Branch  
Department of Infrastructure, Planning and Environment  
PO Box 30  
Palmerston NT 0831  
Australia

Phone: (08) 8999 4414  
Fax: (08) 89999 3666

*Photograph front cover:*  
*Photograph back cover:*

*Aerial view of sinkhole in Cutta Cutta Natural Park, 1994*  
*Sinkhole between Stuart Highway and old North Australia  
Railway line, 1994*

# CONTENTS

EXECUTIVE SUMMARY .....	V
RECOMMENDATIONS .....	VI
1 INTRODUCTION.....	1
1.1 General .....	1
1.2 Objectives of the study.....	1
1.3 Location of the study area.....	3
1.4 Regional climate .....	3
1.5 Geology of the study area .....	4
1.6 Karst.....	4
1.7 Karst landforms.....	5
1.7.1 Surface landforms .....	5
1.7.2 Sinkholes.....	10
1.7.3 Sinkholes in the Katherine region.....	12
1.8 Caves.....	15
1.9 Hydrology of karst landscapes.....	15
1.9.1 Karst aquifer.....	16
2 METHODS AND INFORMATION SOURCES.....	17
2.1 Springs .....	17
2.2 Sinkhole detection.....	17
2.3 Size and shape analysis.....	17
2.4 Relationship between sinkhole development and topographic factors .....	18
2.5 Use of shallow geophysical techniques .....	19
3 RESULTS.....	19
3.1 Springs .....	19
3.2 Sinkhole detection.....	22
3.2.1 Map and image analysis.....	22
3.2.2 Geophysical techniques .....	23
3.3 Sinkhole size and shape analysis .....	23
3.4 Lithologic controls on sinkhole development.....	28
3.5 Polje .....	31
3.6 Historical information about sinkholes in the study area.....	35
3.7 Sinkhole locations.....	37
3.8 Relationship between sinkhole development and topographic factors .....	39
3.9 Comparison of sinkhole development to depth to the water table.....	41
4 DISCUSSION .....	43
4.1 Search for surface signatures of newly-forming sinkholes.....	43
4.2 Water table fluctuations .....	43
4.3 Sinkhole collapse causes.....	44
4.4 Determine the effect of man's activities on sinkhole development.....	47
5 CONCLUSIONS.....	47
5.1 General.....	47

5.2	Further investigations.....	48
5.3	Remedial protective measures for sinkholes.....	49
6	ACKNOWLEDGMENTS.....	49
7	REFERENCES.....	50
8	GLOSSARY.....	51
	Appendix A      Water Quality Data for Springs	
	Appendix B      Morphometry of sinkholes	

## Figures

Figure 1	Location map for the study area .....	2
Figure 2	Average monthly rainfall, Katherine .....	3
Figure 3	Annual rainfall for Katherine (water year October – September) .....	3
Figure 4	The comprehensive karst system: a composite diagram illustrating the major phenomena encountered in active karst terrains (Ford and Williams, 1992).....	6
Figure 5	Principal generic classes of sinkholes (Jennings, 1971).....	11
Figure 6	Schematic diagram showing mechanisms responsible for a sinkhole collapse similar to the one located in Katherine North (AMG co-ordinate 53L 201649-8399429) .....	13
Figure 7	Schematic diagram showing mechanism of sinkhole collapse similar to those observed along the Stuart Highway south of Katherine (AMG co-ordinate 53L 225101-8389338).....	14
Figure 8	Conceptual model of karst aquifer (Doefflinger & Zwahlen 1995).....	16
Figure 9	Measurements made to estimate the two-dimensional geometry of sinkholes Williams (1971).....	18
Figure 10	Hydrograph and chemograph of the CSIRO/Hot Spring G8140312 at AMG co-ordinate 53L 203800-8397300 .....	20
Figure 11	Hydrograph and chemograph of the Northern Bank Spring G8145358 at AMG co-ordinate 53L 203528-8397324 .....	20
Figure 12	Hydrograph and chemograph of the Springvale Spring G8140317 at AMG co-ordinate 53L 201615-8395300 .....	21
Figure 13	Springs flow for G8140312, G8145358, G8140317 and rainfall data obtained during the 1998-2001 .....	21
Figure 14	Rose diagrams showing frequency of distribution of: a) sinkhole long axes orientation, b) Cutta Cutta Cave guiding fractures, c) lineaments from the geological map, d) Tindall Cave guiding fracture, e) lineament from the topographical map.....	24
Figure 15	Sinkhole frequency-depth distributions for six karst regions. These data were fitted to the equation $n = N_0 e^{-kd}$ to obtain the fitting coefficients listed in Table 1.....	25
Figure 16	Depth-rank relationship for 283 sinkholes in the Tindall karst .....	26
Figure 17	Map of sinkhole size classes in Katherine study region .....	27
Figure 18	Stratigraphy of the Tindall Limestone (Lau 1981). The sinkholes and caves are developed in unit L1 and L2 .....	29
Figure 19	Relation between thickness of overburden and sinkhole distribution and location. 30	
Figure 20	Diagram of base-level polje at Lake Hickey. The low water table represents the dry season water table level while the high water table represents the wet season water table .....	31
Figure 21	Map of the sampling points along the two transects across the inundated polje (Lake Hickey) and Dissolved Oxygen concentration contours (13-14.02.2001) at depth 0.1m (surface).....	33

Figure 22 Dissolved Oxygen concentration contours in Lake Hickey (13-14.02.01) at depth 2.5m.....	34
Figure 23 Map showing sinkhole distribution in the study area .....	37
Figure 24 Histogram and cumulative frequency of nearest-neighbour distances of sinkholes in Tindall Limestone. The mean distance = 539 m; median = 404 m; Stan.dev = 454 m ..	38
Figure 25 Nearest neighbour and Poisson distribution of sinkholes in the study area.....	38
Figure 26 Map showing sinkhole distribution in relation to elevation .....	40
Figure 27 Variation in groundwater level in Tindall Limestone in Katherine study area.....	41
Figure 28 Water table in limestone in the study area .....	42
Figure 29 Diagram showing evolution of a sinkhole AMG co-ordinate 53 L 22725008385500. Growth is calculated in Table 3.....	46

## Tables

Table 1 Sinkhole depth distributions in various regions .....	26
Table 2 Historical information about formation of sinkholes in the study area.....	36
Table 3 Growth of the sinkhole located along the fence on the southern part of Cutta Cutta Nature Park, since formation in 1993.....	45

## Plates

Plate 1 Quarry in the Tindall Limestone with visible bedding planes, solution enlarged vertical joints and caves filled with red soil .....	5
Plate 2 Limestone pavement partially surrounded on the left and below by pinnacles .....	6
Plate 3 Clints and grikes in the Tindall Limestone .....	7
Plate 4 Pinnacle karst in thick-bedded to massive limestone.....	7
Plate 5 Pinnacle karst in Cutta Cutta Nature Park.....	8
Plate 6 Tindall Limestone ridge northwest of Cutta Cutta Cave.....	8
Plate 7 Rillenkarrren forms on the Tindall Limestone northwest of Cutta Cutta Caves .....	9
Plate 8 Satellite image showing a polje (black area, top) flooded in March 1998, located north of Katherine town between Stuart Highway, Zimin Drive and Florina Road.....	10
Plate 9 Example of a sinkhole formed by cave roof collapse, located north of Zimin Drive and east of Florina Road .....	12
Plate 10 Example of suffosion sinkhole formed in Cutta Cutta Nature Park (AMG co-ordinate 53L 227250-8385500).....	13
Plate 11 Sinkhole located at AMG co-ordinate 53L 225101-8389338 between the old North Australia Railway embankment and Stuart Highway .....	14
Plate 12 Main corridor in Cutta Cutta cave. The person in the centre is indicating the maximum water level recorded in the cave corridor on 3/03/1973.....	15
Plate 13 Tindall Limestone south of Tindal RAAF Based showing sinkholes; a) filled with water, image captured 27.03.98, b) the same terrain during the dry season (scale 1:100 000).....	22
Plate 14 Polje in the Katherine region (Lake Hickey). Photograph taken on 14 March 2001 during a helicopter reconnaissance .....	31
Plate 15 Sinkhole at AMG co-ordinate 53L 217570-8386610 located south of Tindal RAAF Base (photo taken 16 August 2000, dry season). It represents a sinkhole with an impervious bottom and may hold water throughout the year.....	44

## List of Maps

Sinkholes of the Katherine Region, 1:50 000 scale *in pocket*

Land Units and Sinkholes of the Katherine Region, 1:50 000 scale *in pocket*

## Executive Summary

This project includes the first comprehensive description of sinkholes and their characteristics in the Katherine region. The primary objective of this study is to provide basic information and data aimed at enhancing the understanding of karst topography as it relates to the potential for sinkhole collapses. The project started in July 1999 and was funded jointly by the National Landcare Program and the Northern Territory Government. Its purpose is to provide the Northern Territory Government Departments and Katherine regional authorities and communities with an overview of karst landscape problems, with particular emphasis on sinkhole collapses.

Soluble, karstic rock terrains (limestone) underlie Katherine town and the surrounding region. Agricultural and industrial development and urbanisation of these terrains poses numerous engineering, environmental and planning problems. Such development may change local hydrological regimes and increase the frequency and magnitude of sinkhole flooding and the probability of collapse.

Many sinkholes were formed prior to human settlement in the Katherine region. During the study period, a database of existing sinkholes was established. This assists the continued search for new sinkholes or surface signatures of newly forming sinkholes. During field reconnaissance fresh scarps on sinkholes near Cutta Cutta Nature Park demonstrate recent subsidence or collapse. Also, new sinkhole collapses related to the ponding of rainwater were located in the grounds of Katherine NT Katherine Rural College and along the Stuart Highway.

New sinkholes were located from the air during the helicopter reconnaissance in 1994 and 2001. Based on this, it is clear that acquisition of aerial photography repeated through time at a site of interest is an effective method to detect newly forming sinkholes. Many early surface changes not noticeable from the ground can be easily observed using aerial photography.

The study of sinkholes in the Tindall Limestone shows that present sinkhole collapses are often induced or accelerated by human activities. Triggering mechanisms include:

- changes in the surface flow regime due to road and railway construction
- water ponding due to road and subdivision construction
- leaky water and sewer lines
- major floods (e.g. 1998)
- land clearing for agriculture

Observations of specific sinkholes in the Katherine region generated a set of recommendations that are included in this report and should be consulted in conjunction with this summary.

**Recommendations**

- (1) The water quality of springs in the Katherine region should be assessed by the use of deployable probes and remote loggers (Section 4).
- (2) A water table (piezometric surface) map should be made for any area of concern and water levels in bores monitored.
- (3) Further systematic studies of sinkhole formation in the Katherine region should be undertaken including detailed investigation of triggering mechanisms. These studies are detailed in the conclusions (Section 6).
- (4) A protection zone (100 m diameter?) should be established around sinkholes. Sinkholes behave as stream sinks and can carry pollutant directly to aquifers.
- (5) Changes in local surface drainage due to specific construction activities should be carefully considered and investigated in their individual context as possible sinkhole-collapse triggers.
- (6) Sinkholes should not to be filled with rubbish, soil or closed unless necessary.
- (7) Stormwater drainage should be diverted away from sinkhole openings.

# **1 INTRODUCTION**

## **1.1 General**

A catastrophic flood, which devastated the town of Katherine in January 1998, focused the attention of the Commonwealth and Northern Territory Governments on the region. This natural phenomenon occurred on an unexpected scale causing millions of dollars of damage to property in the town and requiring disaster relief agencies to commit massive resources to the region. The flood itself had a return period of 1 in 155 years. One of the significant outcomes of this was recognition of the importance of scientific information and field observations in understanding the significance of major floods or droughts and the repercussions of these phenomena to the local community and to broader development issues in the Northern Territory.

Following the flood, several projects were proposed for the Katherine region associated with funding available from the National Heritage Trust Program (formerly the National Landcare Program). Most of these proposals emphasised the need to raise awareness within the community, upgrade information and collect more data on flood warning systems, water resources, geology, climate, vegetation and soil. Of particular importance is the potential for sinkhole formation in the Katherine region due to seasonal hydrological factors emphasised by the aforementioned flood. Sinkholes may be described as depressions that occur in the ground surface due to factors associated with underlying geology. They are particularly important in areas where karst topography is a predominant component of the surface or near-surface geology. Karst topography is formed on limestone by dissolution of the limestone material. This dissolution is characterised by the formation of caves and conduits associated with underground drainage and the subsequent formation of sinkholes caused by ground-surface realignment due to its collapse into such caves and dissolution voids.

Soluble, karstic rock terrains (limestone) underlie Katherine town and the surrounding region. Agricultural and industrial development and urbanisation of these terrains pose numerous engineering, environmental and planning problems. Such developments may change local hydrological regimes and increase the frequency and magnitude of sinkhole flooding and the probability of collapse. Sinkhole development associated with carbonate rock is a well-recognised problem in many regions of the world. Ford discusses the increased probability of sinkhole formation following floods or droughts in various limestone regions of Europe, America and Asia (Ford and Williams, 1992).

## **1.2 Objectives of the study**

The primary objective of this study is to provide basic information and data aimed at enhancing the understanding of karst topography as it relates to the potential for sinkhole collapses in the Katherine Region. The project started in July 1999 and was funded jointly by the National Landcare Program and the Northern Territory Government. Its purpose is to provide the Northern Territory Government Department and Katherine regional authorities and communities with an overview of karst landscape problems, with particular emphasis on sinkhole collapses. This information is extremely important for planning processes and is essential to agencies responsible for planning, zoning, design, and construction in areas underlain by the Tindall Limestone.

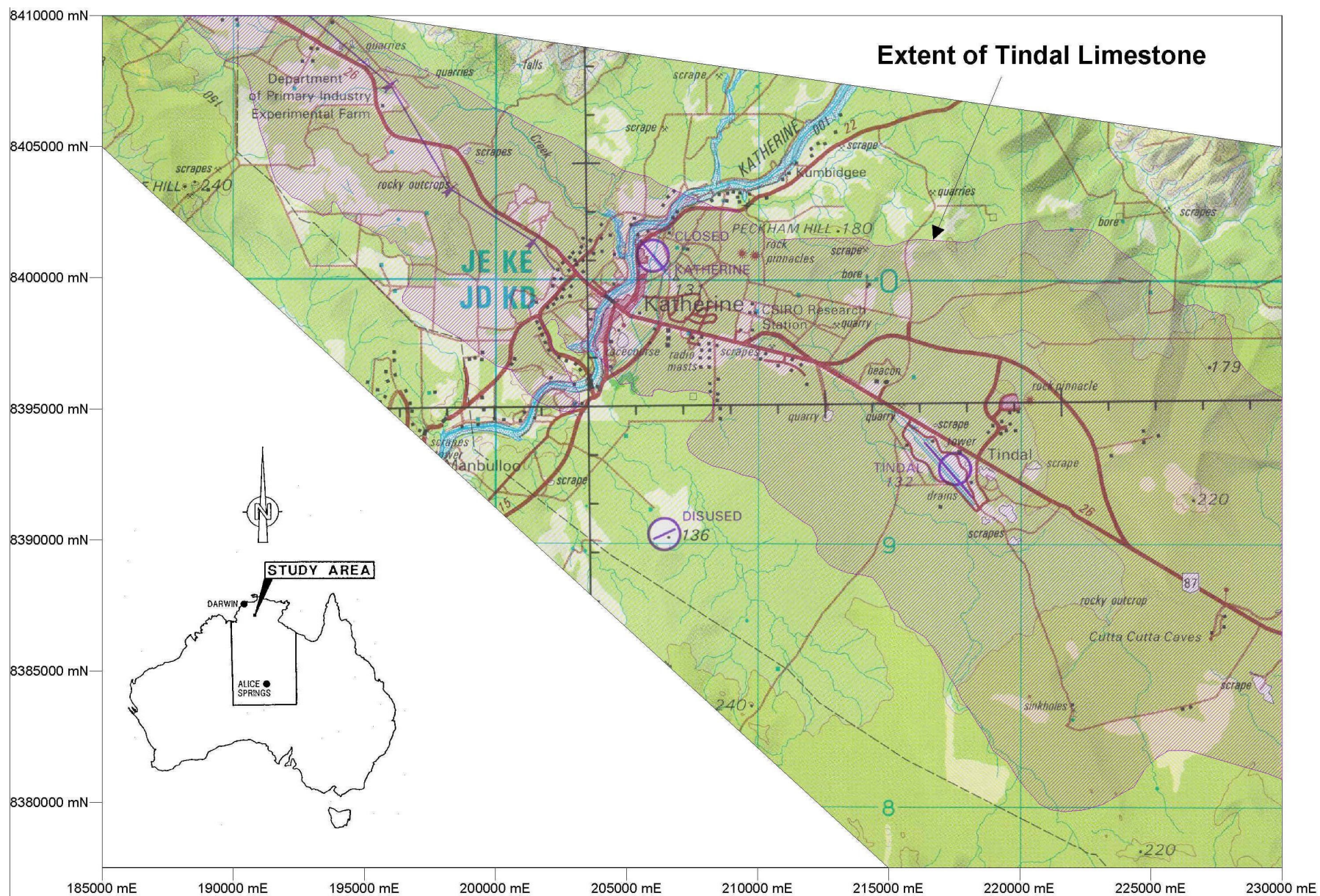


**Figure 1** Location map for the study area

### 1.3 Location of the study area

The study area covers approximately 962.5 km<sup>2</sup>. It extends along the rim of the Daly Basin from Northern Territory University NT Katherine Rural College Campus to the north and to Cutta Cutta Nature Park to the south. The study area is shown in Figure 1.

### 1.4 Regional climate

The study area is located in the wet-dry tropics of Northern Australia. This region has two distinct seasons with a dry season between April and October and wet from November to March. Daily rainfall has been recorded at Katherine since 1873 and is archived with the Commonwealth Bureau of Meteorology. The mean annual rainfall for Katherine is 972 mm. Rainfall is highly seasonal with the vast majority falling in the wet season between October and March. The months of June to August are virtually rainless. Average monthly rainfall and annual rainfall are shown in Figures 2 and 3.

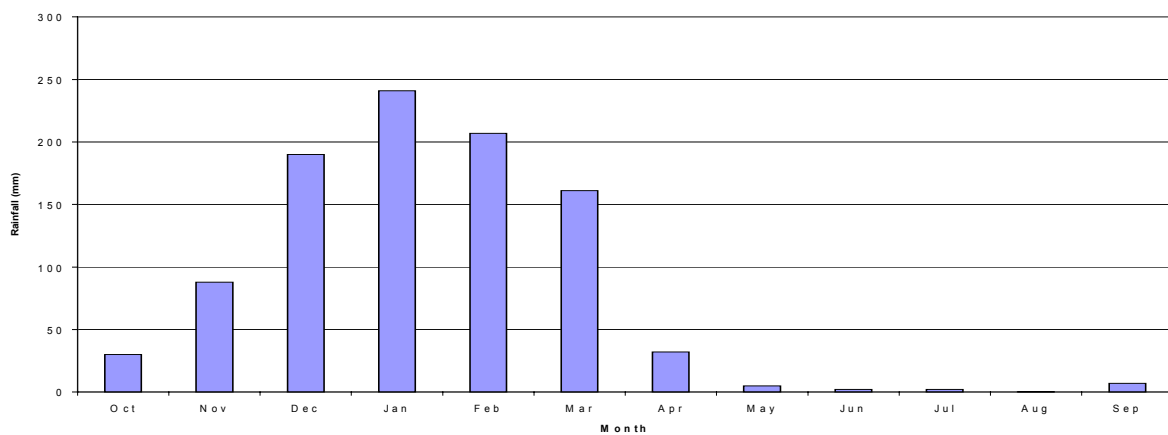


**Figure 2** Average monthly rainfall, Katherine

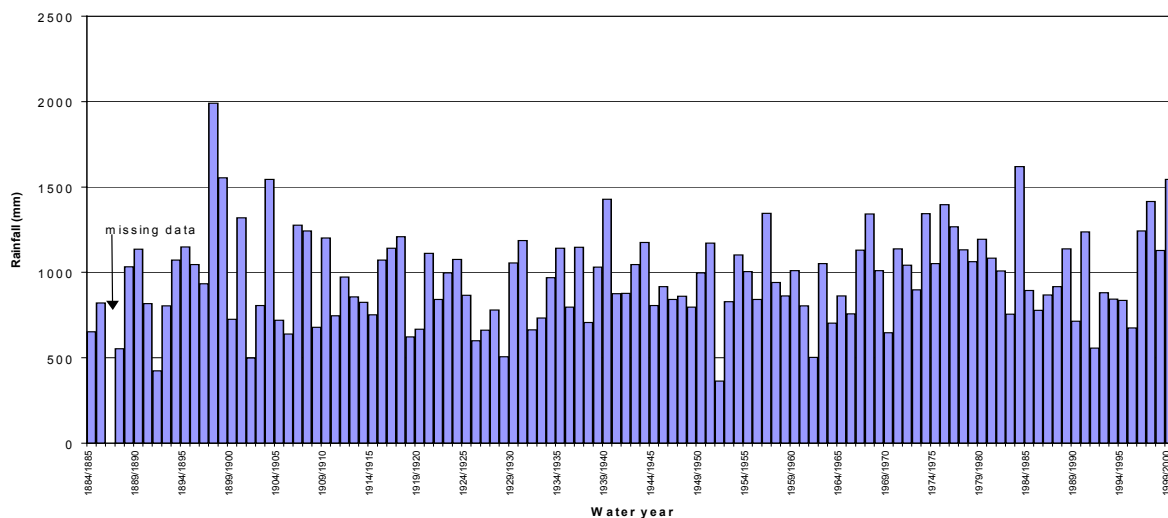


**Figure 3** Annual rainfall for Katherine (water year October – September)

Air temperature ranges from a mean annual maximum of 34<sup>0</sup>C to mean annual minimum of 20<sup>0</sup> C. Evaporation is high, averaging 2279 mm per year, with monthly evaporation exceeding monthly rainfall in 9 month of each year (data from Katherine Research Station No 014910).

## 1.5 Geology of the study area

The study area is located within the eastern rim of the Daly Basin. The Daly Basin is a broad shallow intracratonic structural basin which rests disconformably on Early Cambrian volcanics or unconformably on Early-Middle Proterozoic rocks and includes flat-lying sediments of the Daly River Group. The group consists of the Tindall Limestone, the basal unit, overlain by the Jinduckin Formation, which is in turn overlain by the Oolloo Dolostone. The age of the group ranges from Middle Cambrian to Early Ordovician and attains a maximum measured thickness of 708.5m (drillhole NTGS 86/1). The Daly Basin Group is unconformably overlain by the lower Cretaceous sediments of the Mullaman Beds. The formation in the study area is extensively represented south east of Katherine town toward the town of Mataranka (some 100 km south of Katherine).

Katherine town lies on the rim of the Daly Basin and is enveloped by the Tindall Limestone composed mainly of carbonate sediments. The Tindall Limestone forms a flat-lying unit of grey mottled, onkoid, ribbon and bioclastic limestone with minor intercalations of maroon-green siltstone or dark grey mudstone (Kruse, 1994). The formation attains a maximum known thickness of 182.8m in a drill-core obtained from CCVHI (RN 9058) located at AMG co-ordinate 53L 194800-83 88400. The carbonate, represented mainly by limestone broadly outcropping in the Katherine region, forms landforms described as karst.

## 1.6 Karst

The term “karst” is used by geologist to describe terrain where the bedrock is usually composed of limestone or dolomite (carbonate rocks) and has been, or has the potential to be, easily dissolved by surface water or groundwater. These terrains have distinctive hydrology and landforms arising from a combination of high rock solubility and well-developed secondary porosity. Karst topography is characterised by sinkholes, caves, springs, streams that disappear underground and well-developed subsurface drainage. An important aspect in karst regions is the development of its unique subsurface hydrology.

Karst covers large areas in all continents and in many countries with many cities and communities located on this terrain. It is estimated that karst-waters supply 25% of the global population (Ford and Williams, 1992). At the same time, these communities are vulnerable to particular problems related to karst terrain. These include the design and construction of foundations and structures as well as other activities such as waster disposal and water management.

## 1.7 Karst landforms

Karst topography is characterised by sinkholes, caves, depressions and well developed subsurface drainage. Karst development requires a considerable thickness of carbonate rock. For this reason, karst forms are developed in the Tindall Limestone and Oolloo Dolostone but not in the Jinduckin Formation of the Daly Basin. The weathering of limestone results in the development of void spaces along horizontal bedding planes (resulting in caves), and solution-enlarged, generally vertical joints (fractures), in the bedrock. Solution enlarged joints are the major vertical pathways connecting sinkholes with cavernous zones (caves) in the bedrock beneath the surface. In some places, areas of joint intersection in the bedrock (in the vertical plane) are prime localities for sinkhole initiation on the surface. Examples of these processes are evident in Plate 1.

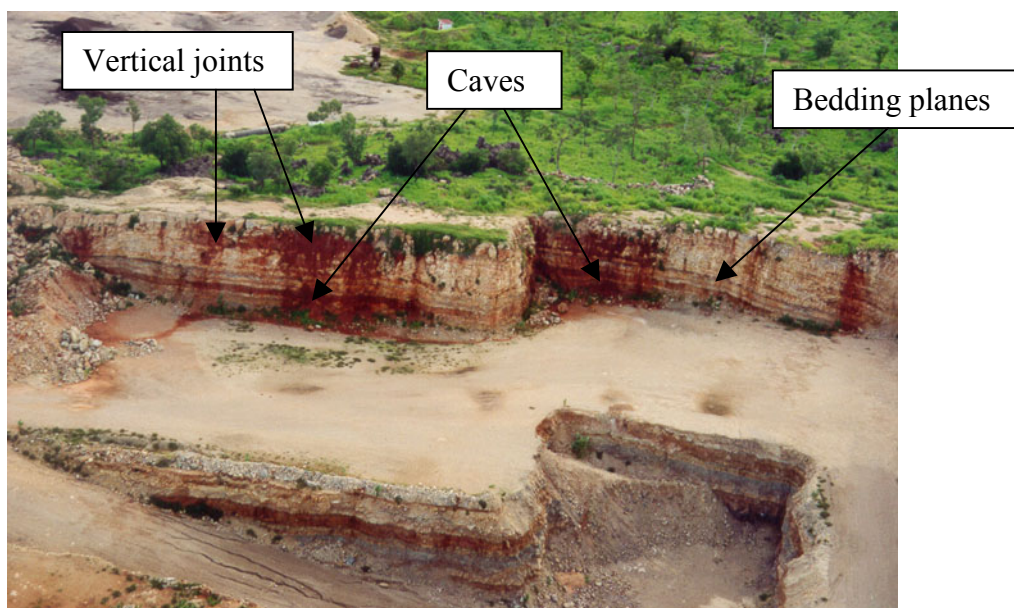


**Plate 1** Quarry in the Tindall Limestone with visible bedding planes, solution enlarged vertical joints and caves filled with red soil

### 1.7.1 Surface landforms

Karst landscape extends north and south of Katherine along the limestone rim of the Daly Basin. While the explanation of the physical and chemical development of this karst is complex, what follows is a relatively basic description of some development mechanisms and different forms of karst.

Figure 4 illustrates the relation between the main features of a karst system. The system may be divided into erosional and depositional zones. The karst forms in this study are predominantly located in the erosional zone of the Tindall karst system.

Large numbers of outcrops in the Tindall Limestone consist of pavement karst with small to wide grikes. In some places the heavily dissected surface is replaced with pinnacles or small towers. Plate 2 shows a photograph of limestone outcrops taken from a helicopter north of

Katherine town. In this photograph the clint-and-grike morphology is clearly visible. It occupies the central parts of the outcrop and the pinnacles form an interface to the surrounding alluvial plains.

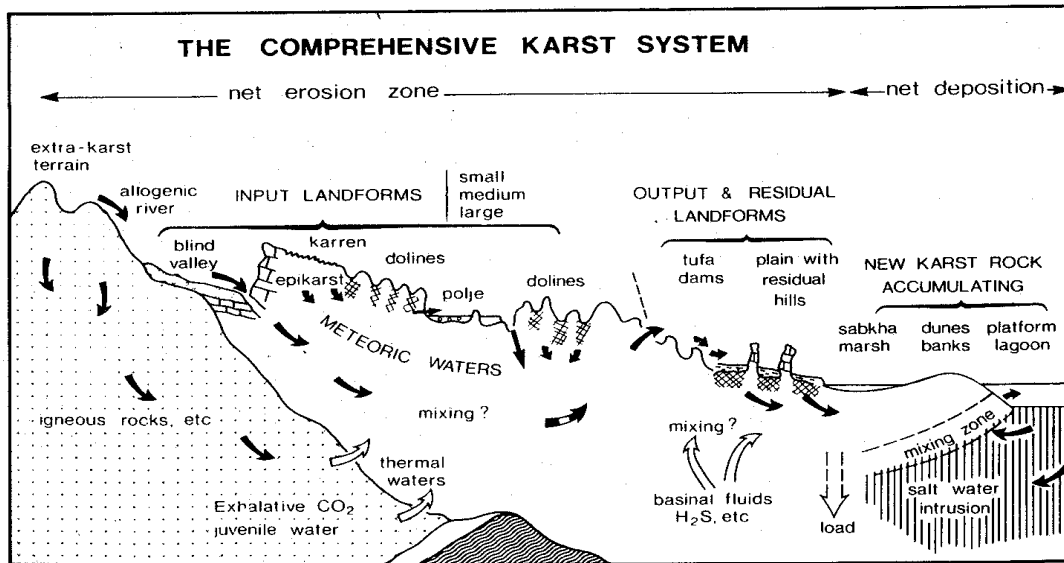


**Figure 4** The comprehensive karst system: a composite diagram illustrating the major phenomena encountered in active karst terrains (Ford and Williams, 1992)

The limestone pavement can be described as a bare plane surface of limestone, parallel to the bedding, commonly divided into blocks (clints) by solutionally widened joints (grikes). A close-up of the pavement is shown in Plate 3. Clearly visible grikes and clints. Grikes form solution enlarged vertical joints in the surface of a karst-land, extending for up to a few meters into the limestone. Clints show up as slabs of limestone, parallel to the bedding and form a horizontal pavement with widened joints, isolate individual clints.

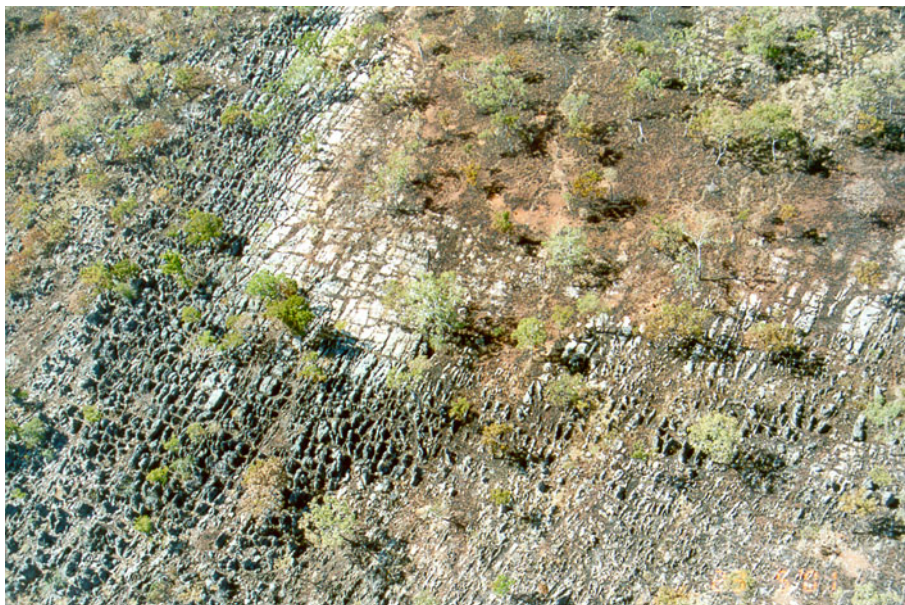


**Plate 2** Limestone pavement partially surrounded on the left and below by pinnacles



**Plate 3** Clints and grikes in the Tindall Limestone



**Plate 4** Pinnacle karst in thick-bedded to massive limestone

Reliefs composed of karst pinnacles are shown in Plates 4 and Plate 5 with Plate 6 showing a limestone ridge in the Cutta Cutta cave region.



**Plate 5** Pinnacle karst in Cutta Cutta Nature Park



**Plate 6** Tindall Limestone ridge northwest of Cutta Cutta Cave

‘Karren’ is a particular formation that develops on bare limestone surfaces. It is formed by the dissolution of the limestone by surface flow and may take a number of forms. Karren is well developed on the exposed surface of the Tindall Limestone. The specific nature of karren development depends on subtle differences in rock lithology. Karren can be variously classified; the most common is rillenkarren. Rillenkarren forms shallow channels separated

by sharp ridges 2-3 centimetres apart. This is common in the Cutta Cutta Nature Park area and is shown in Plate 7.



**Plate 7** Rillenkarren forms on the Tindall Limestone northwest of Cutta Cutta Caves

‘Polje’ is a term to define flat, enclosed depressions in karst terrain. Polje is associated with input or throughput of water. Several authors differ in their strict definition of polje. In this report the description provided by Gams (1978) is used. He includes three primary criteria to define a polje. These are:

- Flat (or terraced) floor in rock or in unconsolidated alluvium.
- A closed basin with a steeply rising marginal slope on at least, one side.
- Karstic drainage

A satellite image of the polje known as Lake Hickey is shown in Plate 8.



**Plate 8** Satellite image showing a polje (black area, top) flooded in March 1998, located north of Katherine town between Stuart Highway, Zimin Drive and Florina Road

### 1.7.2 Sinkholes

Karst geomorphologists pay special attention to sinkholes and identify them as primary-index karst landforms (Ford and Williams, 1992).

**Sinkhole or doline?** The terms sinkhole and doline are synonymous. In this report the simple descriptive term in English “sinkhole” is used instead of “doline”. In North American literature (e.g. Beck 1984) the word “sinkhole” is used to describe enclosed depressions caused by dissolution of the underlying rocks, i.e. karst processes. However since the Anglo-American words “sinkhole”, “swallow hole” and “swallet” have been used very loosely, the word “doline” has been preferred by many American karst scientists. Doline is derived from south Slav languages and means any depression in the landscape.

**What is the sinkhole?** A sinkhole can be broadly defined as a closed depression in the land surface, generally elliptical to circular in areal view, with internal drainage. It results from the downward movement or collapse of surface material into solution openings of the underlying carbonate rock. Formation of sinkholes is part of the natural weathering process and their development requires a landscape underlain by soluble rock such as limestone, dolomite, rock salt or gypsum. Some sinkholes form slowly by solution of the underlying rock; other sinkholes develop as a result of a collapse of surface or near surface material. Diagrams of the major types of sinkhole are presented in Figure 5.

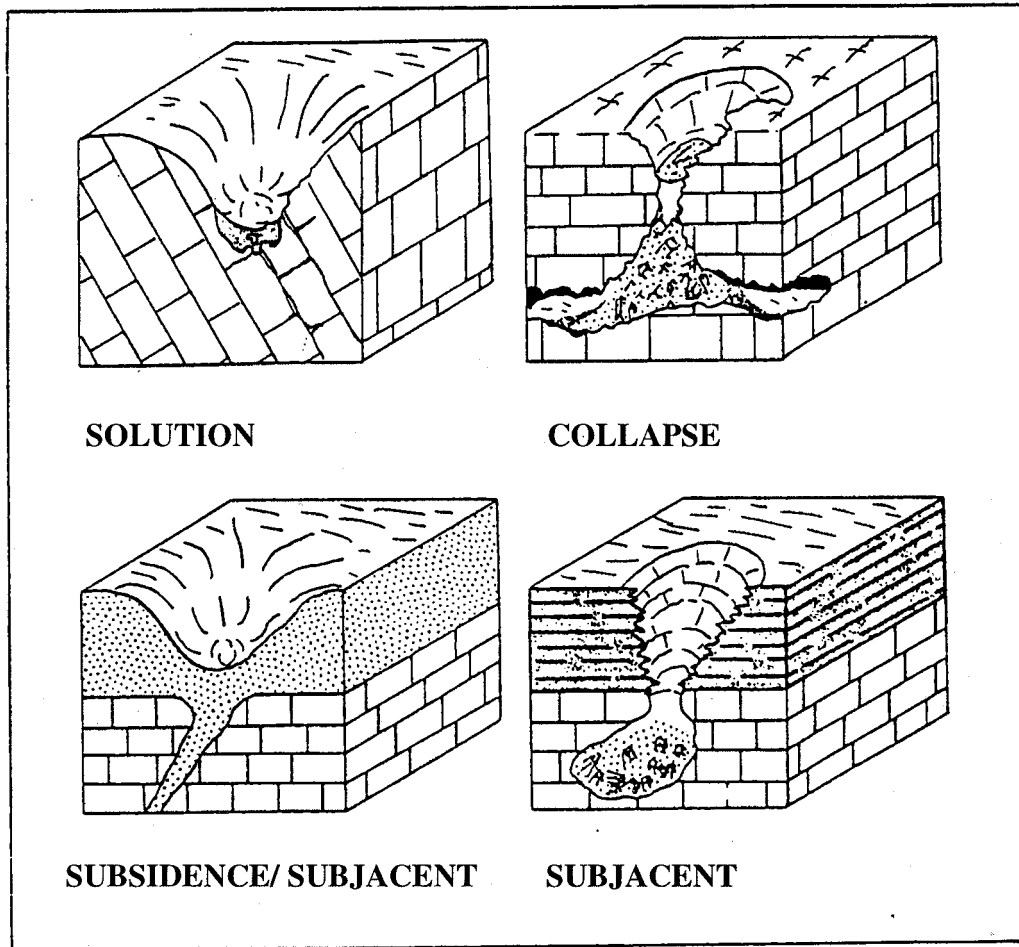


**Figure 5** Principal generic classes of sinkholes (Jennings, 1971)

**Solution sinkholes** are depressions in the bedrock surface formed by a gradual process involving sagging or settling of the surface without obvious breaking of the soil. “These are due primarily to pronounced surface solution of the karst bedrock around some favourable point such as a joint intersection. The solutes and some insoluble residues are removed down the solution-widened planes of weakness, though once the latter are enlarged to shaft dimensions there will be sliding and falling of residues and rock fragments brought to their apertures. As soon as a focus of downward percolation is established by dissolution, it will gather drainage to itself and the embryonic doline will further its own development.” (Jennings, 1971, p 121). This type of sinkhole develops by a slow process and is generally not associated with a high risk of collapse. Solution sinkholes do not generally present significant engineering foundation problems. They may however, cause some settling and associated cracking of foundation material.

**Collapse sinkholes** form by the collapse of the roof of a bedrock cavern. This type of collapse produces a steep sided, bedrock-walled hole sometimes widening into cave passages at depth. This type of collapse is not very common. Of the 650 sinkholes recorded in Florida in recent years only one might be described as a cave roof collapse (Beck, 1984). Nonetheless, damage associated with such catastrophic collapse can be great.

**Subsidence/suffosion sinkholes** form by the deposition of unconsolidated overburden into widened joints and solution pipes in the underlying soluble bedrock. An informative

description of this type of sinkhole is given by Jennings (1971, p. 126). “Where superficial deposits or thick residual soils overlie karst rocks, dolines can develop through spasmodic subsidence and more continuous piping of these materials into widened joints and solution pipes in the bedrock beneath. They vary much in size and shape. A quick movement of subsidence may temporarily produce a cylindrical hole which rapidly weathers into a gentler conical or bowl shaped depression”. This type of sinkhole can form very rapidly. A majority of sinkhole collapses that cause significant damage are in this category. In the Katherine region, the vast majority of sinkholes that have collapsed in recent years belong to this category.

**Subjancet sinkholes** are closed depressions of various shapes and sizes found in other rock formations overlying karst rocks. This category of sinkhole was not observed in the study area.

### 1.7.3 Sinkholes in the Katherine region

Three types of sinkhole were observed in the study area:

- Collapse sinkholes
- Suffosion sinkholes
- Solution sinkholes

Plate 9 shows a typical collapse sinkhole formed on a section of the bare, exposed Tindall Limestone outcrop. A typical suffosion sinkhole is shown in the photograph taken during a helicopter reconnaissance in March 2001 (Plate 10).



**Plate 9** Example of a sinkhole formed by cave roof collapse, located north of Zimin Drive and east of Florina Road

During the field-work only a few sinkholes observed could be classified into one category. That is, as pure collapse, suffosion or solution type. In reality, the vast majority of sinkholes in the Katherine region are hybrids of the above three forms. Of 283 sinkholes studied, only one could be classified as a pure ‘collapse’ type. The rest were representative of

suffosion/collapse and solution /collapse types with slightly more in the suffosion/collapse type. Diagrams of a collapse sinkhole formation are shown in Figure 6. Only one sinkhole of this type was observed in the study area (See Plate 9).

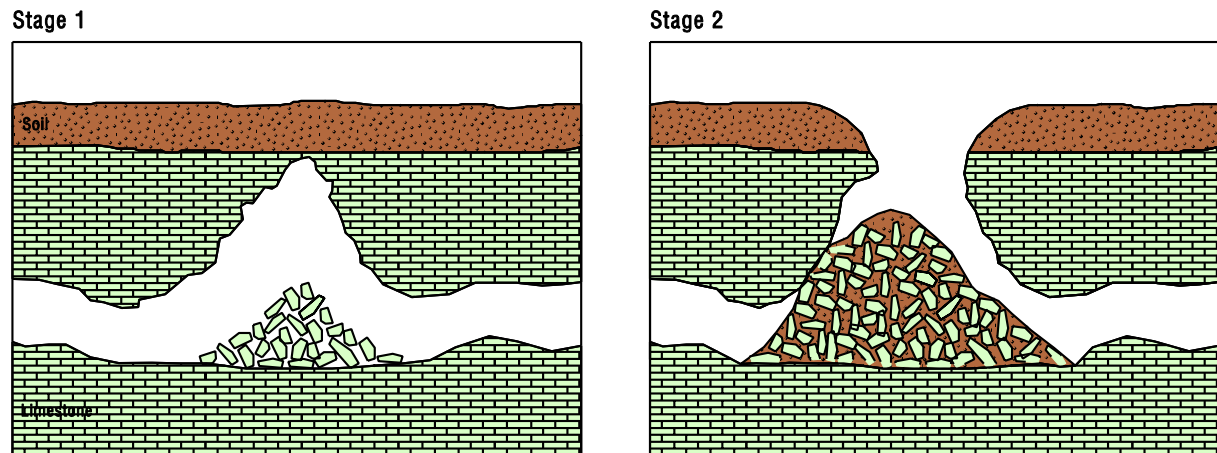


**Figure 6** Schematic diagram showing mechanisms responsible for a sinkhole collapse similar to the one located in Katherine North (AMG co-ordinate 53L 201649-8399429)

The type of collapse shown in the above Figure 6 can be associated with the oscillation of the water table between wet and dry seasons. Temporary backing-up of water in conduits due to flash floods also produces rapid changes in stress patterns in karstified limestone. Seasonal water table fluctuations of up to 13m are known in the Katherine area. Sinkholes so-formed develop from a combination of undermining from below (e.g. cave formation) and periodic removal of buoyant support.



**Plate 10** Example of suffosion sinkhole formed in Cutta Cutta Nature Park (AMG co-ordinate 53L 227250-8385500)

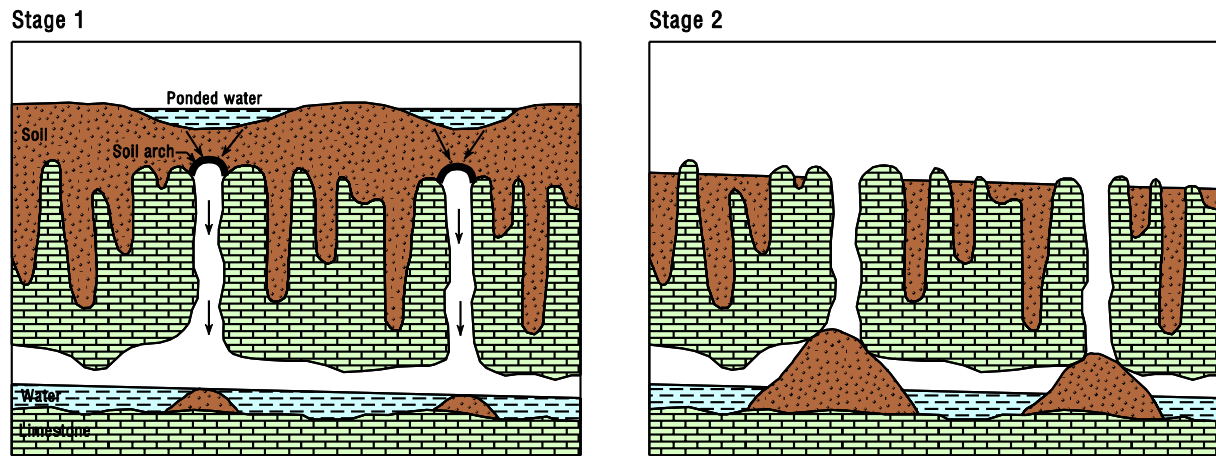


**Figure 7** Schematic diagram showing mechanism of sinkhole collapse similar to those observed along the Stuart Highway south of Katherine (AMG co-ordinate 53L 225101-8389338)

In cases described by Figure 7, the water table is below the soil-bedrock contact. Collapses are usually caused by an increase in downward movement of surface water. Stage 1 in Figure 7 shows surface runoff concentrated in drains and impoundments increasing the downward pressure of water.



**Plate 11** Sinkhole located at AMG co-ordinate 53L 225101-8389338 between the old North Australia Railway embankment and Stuart Highway

This results in the piping of saturated soil into openings in the limestone. Stage 2 shows the collapse of soil arches due to loading of the surface by ponded water or vibration of the surface associated with blasting or road transport. Examples of this types of sinkhole

formation are located between 10 to 50m from the Stuart Highway, some 25km south of Katherine at AMG co-ordinate 53L 225101-8389338 and are shown in Plate 11.

## 1.8 Caves

Caves are the most interesting and spectacular manifestation of karst formations. They are naturally formed subterranean open areas. The Tindall Limestone has a number of well-developed cave systems. The best known are located in Cutta Cutta Nature Park and Kintore Nature Park (Plate 12).



**Plate 12** Main corridor in Cutta Cutta cave. The person in the centre is indicating the maximum water level recorded in the cave corridor on 3/03/1973

## 1.9 Hydrology of karst landscapes

The most important factor affecting karst landscapes is the general hydrologic setting. One of the characteristic features, also observed in the study area, is the absence of perennial surface streams. Drainage networks in karst are developed principally in the subsurface region. They consist of interconnected systems of caves, enlarged vertical fractures and smaller cavities developed along bedding planes. The Katherine River originates outside (east) of the karst landscape but flows across the Tindall Limestone as a perennial stream (See Figure 1). This river serves as the major discharge point for groundwater emanating from the Tindall

Limestone. Data from springs, numerous water bores and observation bores were collected. to better understand the hydrology in the region.

### 1.9.1 Karst aquifer

A conceptual model of a karst aquifer presented below (Doeflinger and Zwahlen, 1995) can be used to characterise the Tindall Limestone aquifer. Karst aquifers are described as anisotropic. This implies that they include a network of conduits with high hydraulic conductivity ( $K > 10^{-1}$  m/s) surrounded by a large volume of low permeability fractured and fissured rock ( $K$  between  $10^{-3}$  and  $10^{-7}$  m/s). Additionally, the karst network can drain water out of surrounding rock or alternatively, recharge it according to the hydrodynamic state of the aquifer. This model shown in Figure 8 is based on specific geomorphologic and hydraulic karst phenomena. These include:

- A general absence of surface drainage. Only streams that develop outside or adjacent to karst terrain will be observed to flow through it (i.e Katherine River); drainage networks are developed principally in the subsurface.
- The existence of large springs (e.g. G8140312, G8140317, G8145358 detailed later in the Section 3.1).
- Sinkholes (see attached map “Sinkholes of the Katherine Region”).
- The existence of networks of karst solution conduits.
- Water levels that may change rapidly and substantially in response to heavy rains (recorded by observation bore RN 32747, RN 22286 and discussed in Section 4.9). Fluctuations in the water levels are of two categories - seasonal and pulse. Seasonally the water level drops during the dry season reaching a minimum in November/December. It starts rising in January to reach a maximum in March.

Sinkholes play an important role in karst hydrology. They act as collecting basins for surface runoff and transfer surface water collected in the depressions drains, vertically through the soil into bedrock fractures. The groundwater recharge in the Tindall Limestone occurs primarily through sinkholes and solution enlarged joint sets.

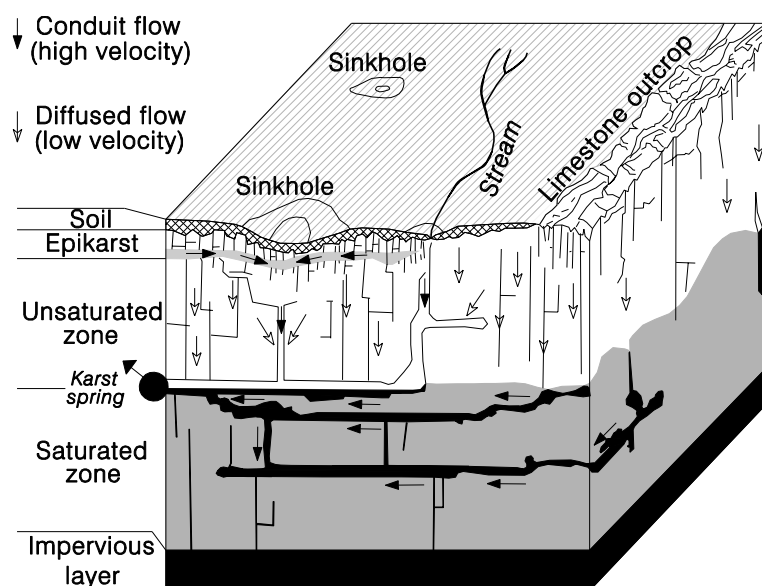


**Figure 8** Conceptual model of karst aquifer (Doeflinger & Zwahlen 1995)

## 2 METHODS AND INFORMATION SOURCES

A range of different methods was used in this project. These are summarised below. Computer programs used in data analysis, map construction etc. are not specifically noted unless they vary from 'standard' commercially available software.

### 2.1 Springs

The present groundwater monitoring network in the Katherine region consists mainly of water bores and three natural groundwater springs (Springvale Spring G8140317, Northern Bank Spring G8145358 and CSIRO /Hot Spring G8140312)

During this two-year study (1999-2001) these springs were sampled and measured to determine the physical and chemical constituents in the groundwater. This information forms a basis for development of a long-term groundwater monitoring and management plan for the groundwater resources in the Daly Basin, with special focus on the Katherine Region. Water samples and flow measurements were collected every month from the springs. Collected samples were analysed at the Department of Business, Industry and Resource Development formally the Resource Protection Division's Water Chemistry Laboratory at Berrimah NT. Determinants measured were:

- a) Physico-chemical parameters (specific electrical conductivity, water temperature, pH)
- b) Alkaline elements and analogues ( $\text{Na}^+$ ,  $\text{K}^+$ ,  $\text{NH}^+$ )
- c) Alkaline earth elements ( $\text{Mg}^{2+}$ ,  $\text{Ca}^{2+}$ )
- d) Carbonate species ( $\text{HCO}_3^-$ ,  $\text{CO}_3^{2-}$ , free carbonic acid)
- e) Inorganic nitrogen compounds ( $\text{NO}_3^-$ ,  $\text{NO}_2^-$ ,  $\text{CN}^-$ )
- f) Environmental markers ( $\text{Cl}^-$ ,  $\text{SO}_4^{2-}$ ,  $\text{PO}_4^{3-}$ )

In this report only hardness and alkalinity are discussed. A complete set of results for all the above determinants is shown in Appendix A.

### 2.2 Sinkhole detection

The primary location of all sinkholes in the project area was determined by use of topographic maps and aerial photographs. Topographical maps in scales 1:5 000, 1:10 000, 1:50 000 and 1: 100 000 were used. All detected sinkholes were transferred onto a 1:10 000 base map. For photo-interpretation the following aerial photographs were used:

- Black and white in scale 1:30 000 flown 24.04.48 cover the whole project area
- Black and white in scale 1:80 000 flown 2.05.62 cover the whole project area
- Colour in scale 1 :25 000 flown 9.06.81 cover the whole project area

### 2.3 Size and shape analysis

Descriptions of the two-dimensional geometry of karst depression depth, width, and elongation trends in sinkholes were determined using measurement protocols described by

Williams (1971). His methods allow a standard technique to be used for sinkholes of various shapes and ensure that comparisons of areal shape between sinkholes are consistent. This method is described in Figure 9.

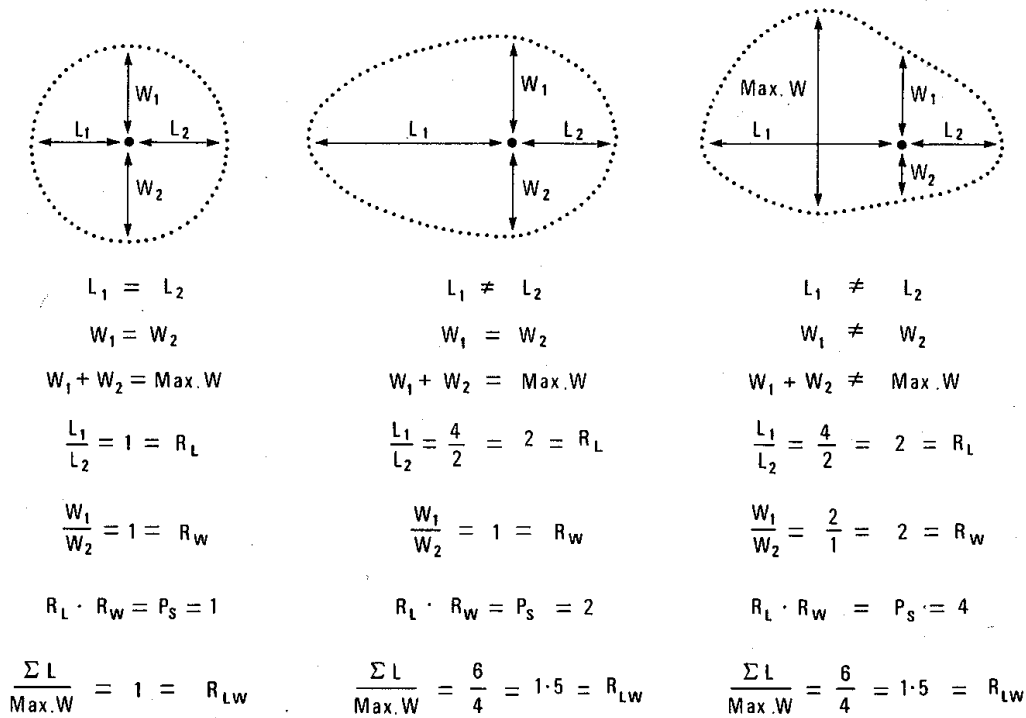


**Figure 9** Measurements made to estimate the two-dimensional geometry of sinkholes Williams (1971)

The width to depth ratio helps distinguish collapse sinkholes from solution sinkholes. If preferred trends of individual sinkhole axes occur or sinkholes are found to align, these orientations should be statistically compared to joint, fracture, fault, and photo-lineament trends to determine the amount of structural control on sinkhole growth.

Analysis of the distribution patterns of sinkholes is discussed by Williams (1972b). This analysis is done in order to determine whether the sinkhole population tends to cluster in some way. Sometimes, sinkholes tend to cluster, either as satellites of smaller sinkholes around major ones, and/or they are clustered along certain structural features, like fractures or fault zones in the underlying bedrock.

## 2.4 Relationship between sinkhole development and topographic factors

Topography is known to affect the development of sinkholes. Therefore, in order to better predict and understand the future occurrence of sinkholes, it was necessary to determine the distribution of sinkholes and sinkhole types with regard to topographic features such as valleys, uplands, etc. This was achieved by overlaying the sinkhole location map ((see attached Map Land Units and Sinkholes of the Katherine Region 1:50 000) on a standard Katherine area map showing landforms, soil, vegetation.

## 2.5 Use of shallow geophysical techniques

During May and June 2000 geophysical surveying was completed in three selected regions. The aim was to delineate subsurface features associated with sinkhole development. Pole-dipole resistivity, electromagnetic (EM34) and ground penetrating (GPR) radar methods were used to delineate filled fractures and sinkholes.

To achieve comprehensive information about sinkhole detection three geologically different terrains were selected for investigation:

- Terrain without soil cover located in Katherine Rural College
- Terrain with soil cover between 0-5m located in Katherine North. This terrain forms a karst depression which can be flooded in the wet season
- Terrain with soil covers greater than 5m located in Cutta Cutta Nature Park.

To corroborate the geophysical observations, drilling was undertaken on nominated targets. On the NT Portion 5189 (Hickey site) thirteen bores intersected the Tindall Limestone to a maximum depth of 67.5m. In the Cutta Cutta region four bores were drilled to a maximum depth of 43.3m. Only one bore was drilled in the Katherine Rural College region and Tindall Limestone was encountered to a depth of 55.2 m. A comprehensive report on the finding of this work was produced (DIPE, Report A. Knapton, 2002 “Geophysics of Karstic Terrains”).

## 3 RESULTS

### 3.1 Springs

Springs flows show discharge variations controlled by rainfall but no significant changes in water quality (alkalinity and hardness) were observed (Figure 10, 11 and 12). It is likely that the frequency of sampling was inadequate to provide data for more comprehensive (discrete) analysis of water quality changes in the Tindall aquifer. Such changes may be detectable if automatic data loggers (recording per hour) were installed in the springs. In summary, the response of aquifer water quality to recharge was not readily detectable from the data collected during this study.

Springs discharge was measured monthly (Figure 13), however during the wet season between December and March, the Katherine River level was above the springs level. Springs are located in the Katherine River Valley only slightly above “dry season” river levels. As result, after December rains, springs are not accessible. As expected, spring flow shows a marked response to rainfall with the biggest flow recorded after the 1998 flood.

From three observed springs:

- G8140312 shows flow between 284 and 555 L/s;
- G8145358 flow between 38 and 55 L/s and
- G8140317 flow between 65 and 297 L/s.

Spring G8140317 shows the biggest response to rainfall whereas G8125358 shows fairly stable flow throughout the year. A few big springs exist in the bed of the Katherine River between the Railway Bridge and Low-Level Crossing but in this investigation, the specific locations of the springs were unknown.

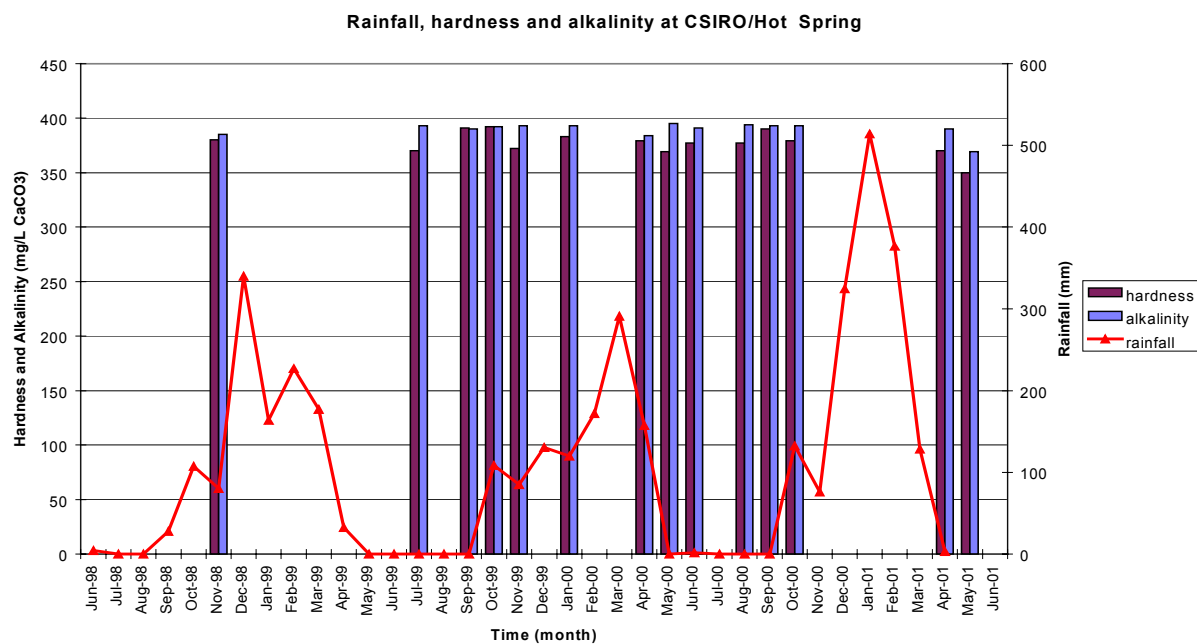


**Figure 10** Hydrograph and chemograph of the CSIRO/Hot Spring G8140312 at AMG co-ordinate 53L 203800-8397300

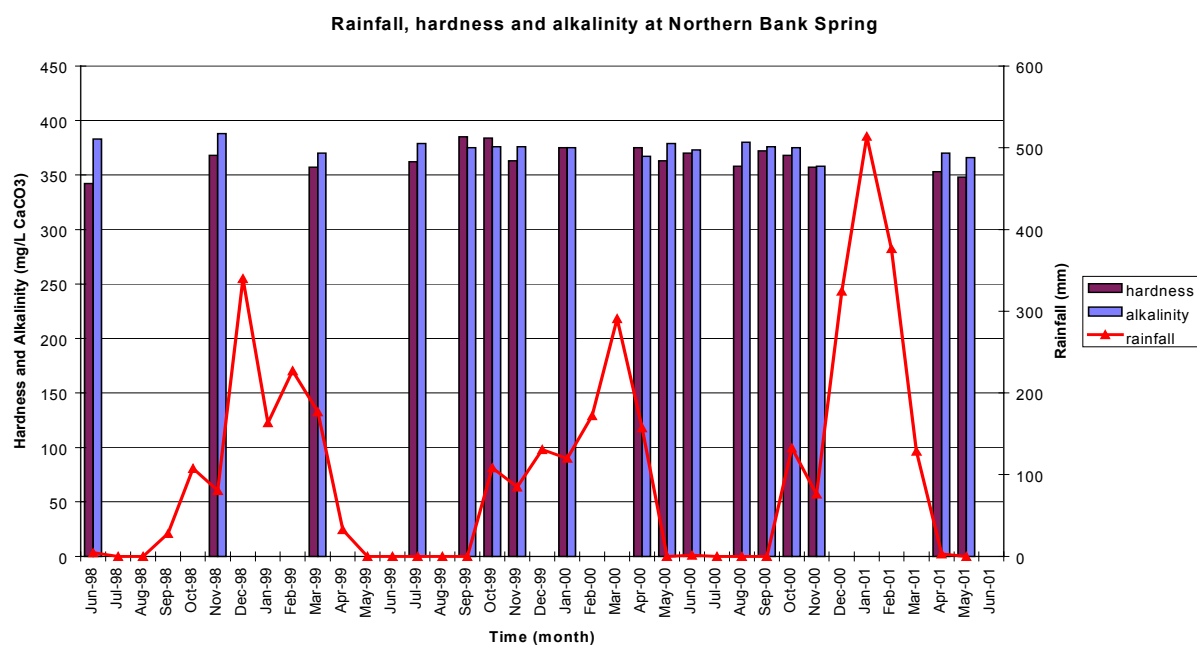


**Figure 11** Hydrograph and chemograph of the Northern Bank Spring G8145358 at AMG co-ordinate 53L 203528-8397324

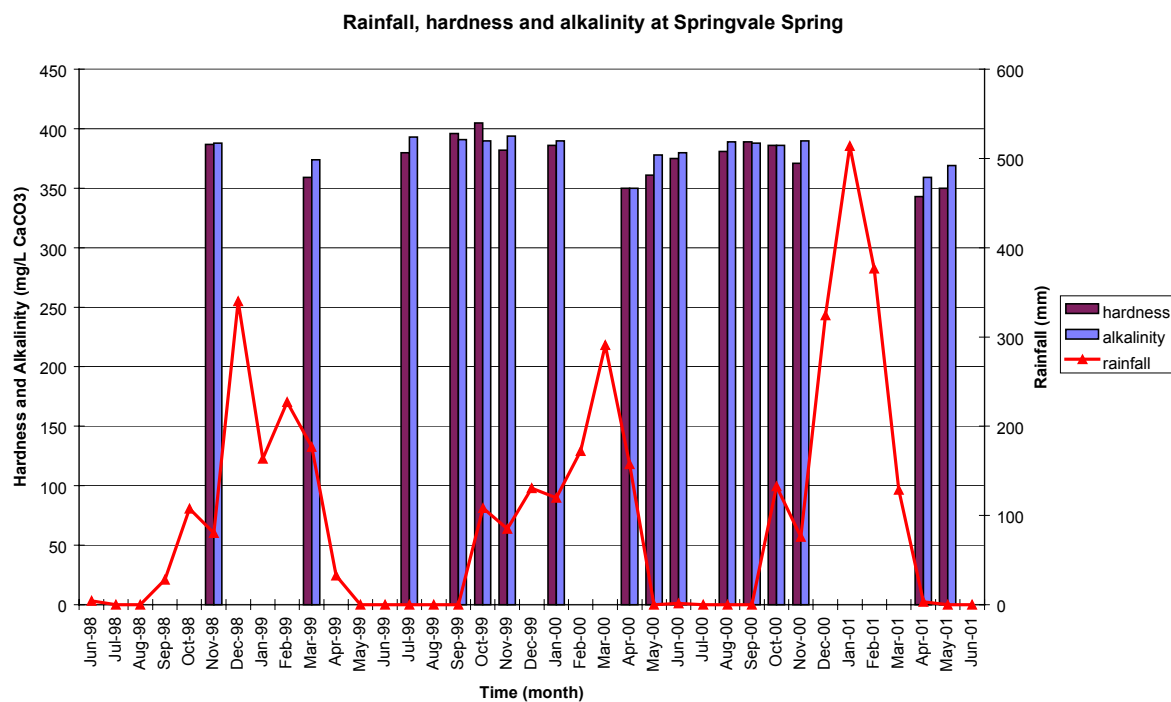


**Figure 12** Hydrograph and chemograph of the Springvale Spring G8140317 at AMG co-ordinate 53L 201615-8395300

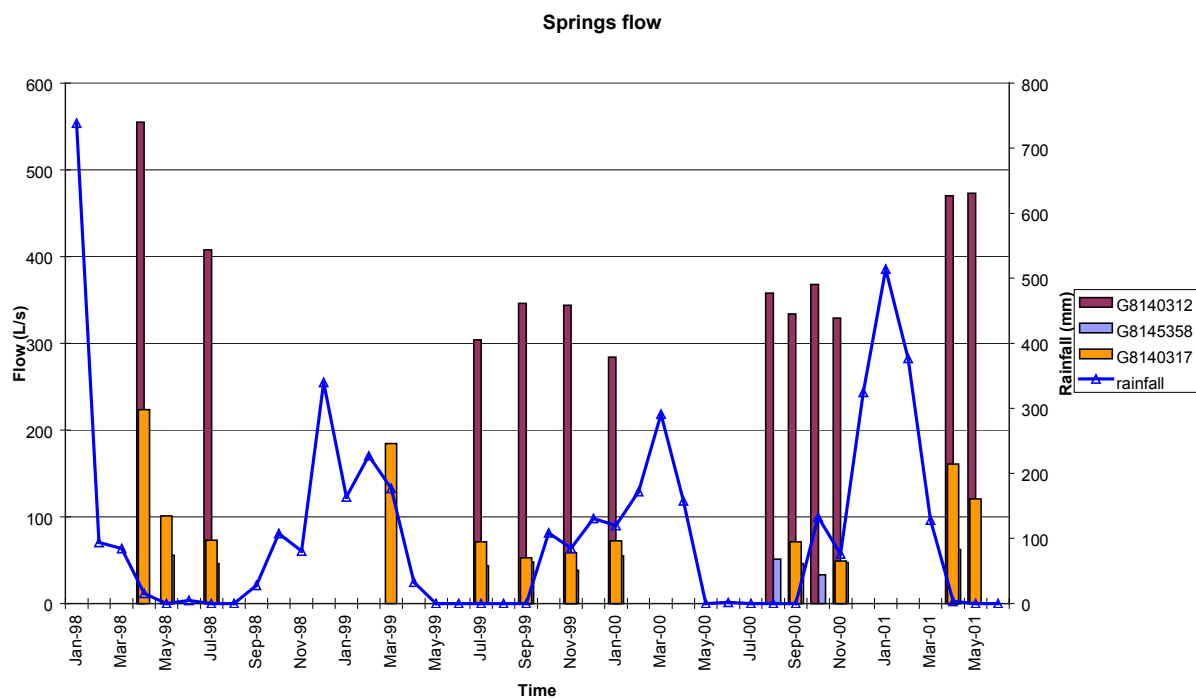


**Figure 13** Springs flow for G8140312, G8145358, G8140317 and rainfall data obtained during the 1998-2001

## 3.2 Sinkhole detection

### 3.2.1 Map and image analysis

The study area is underlain by limestone that exhibits characteristic topographic features of a karst terrain. The most obvious features are the existing sinkholes and solution depressions. These were identified as closed contours from topographic maps (if their depths exceeded the contour interval). They were also identified from stereoscopic examination of overlapping air photographs.

Satellite images (Landsat-5 TM Bands: BGR 345) clearly showed water-filled depressions (Plate 13) or displayed a signature different to the surrounding landscape due to vegetation contrasts. For instance, in the outcrops of bare karst in the Katherine area, cave entrances are often recognised by *Ficus platypoda* trees growing in their entrances due to the more humid environment in them. Once detected, individual sinkholes of significance were also inspected in the field.

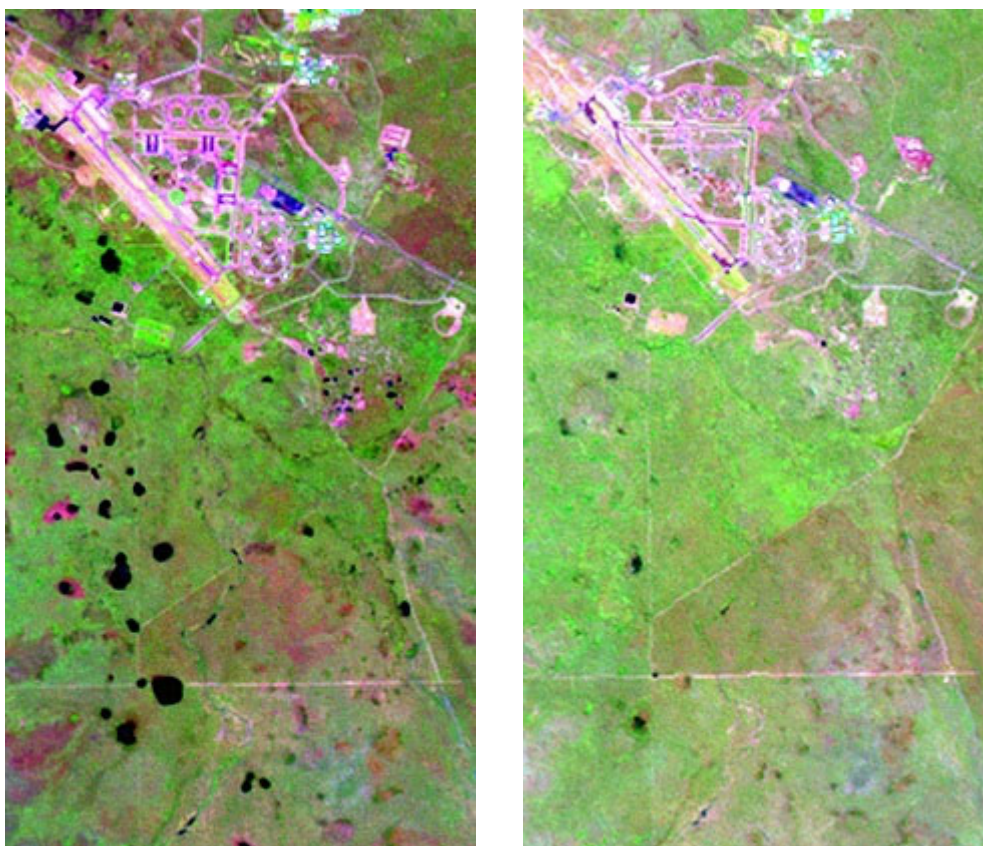


**Plate 13** Tindall Limestone south of Tindal RAAF Based showing sinkholes; a) filled with water, image captured 27.03.98, b) the same terrain during the dry season (scale 1:100 000)

A map of sinkholes in the region was developed and is shown in map “Sinkholes of the Katherine Region in 1:50 000 scale” (see attached).

### 3.2.2 Geophysical techniques

Results obtained with ground penetrating radar (GPR) were encouraging. The detection of sinkholes was generally very successful, due to low electrical conductivities and the high dielectric contrasts between sinkholes and limestone. The major disadvantage of GPR is the limitation in depth investigations in conductive ground and interference from trees.

(Note: GPR surveys should be used in future geotechnical projects in Katherine region only where operators with previous experience in karst terrain can be engaged. It is also very important to use the latest, most modern GPR equipment. This is a relatively new technology and technical progress in equipment is very rapid.)

### 3.3 Sinkhole size and shape analysis

To compare preferred trends of individual sinkhole axes to joint, fracture and fault lineaments data were extracted from the topographical map (Katherine 1:100 000 map sheet 5369) and geological map (Geology of Edith River Region 1:100 000). The lineaments from the topographical map refer to straight lines in the landscape (which are often fracture zones) whereas the fault lineaments on the geological map are interpreted structures. Collected sets of data were analysed by rose diagram shown in Figure 14. The topographical map lineament distribution is different to the fault traces (Figure 14.e and c.). The prominent NNW-SSE trend found in the map lineaments is lacking in the fault sets.

The rose diagrams in (Figure 14.a) display the distribution of the long axes of the 283 sinkholes in their frequency regime. They show a wide selection of axial trends with the dominant trend of the NNW-SSE. This direction is well expressed in the Cutta Cutta and topographical map plot (Figure 14.b and e) and is not as strong in the geological and Tindall Cave rose diagrams (Figure 14.c and d). The analysis described above shows that the orientation of sinkhole long axes is related to structural controls of the Cutta Cutta Caves.

The distribution of sinkhole frequency versus depth for the Tindall Limestone can be compared with analysis completed for six karst regions shown in Figure 15 (White, 1988). The depths of sinkholes in many regions of the world display an exponential distribution of the form:

$$n = N_0 e^{-kd} \quad (1)$$

i.e. the number of sinkholes ( $n$ ) with a depth ( $d$ ) less than the deepest ( $N_0$ ) decay exponentially. Within a sinkhole population, this expression can be converted to an expression for the fraction of sinkholes shallower than the deepest as follows:

$$n / N_0 = e^{-kd} \quad (2)$$

or

$$\ln(n / N_0) = -kd \quad (3)$$

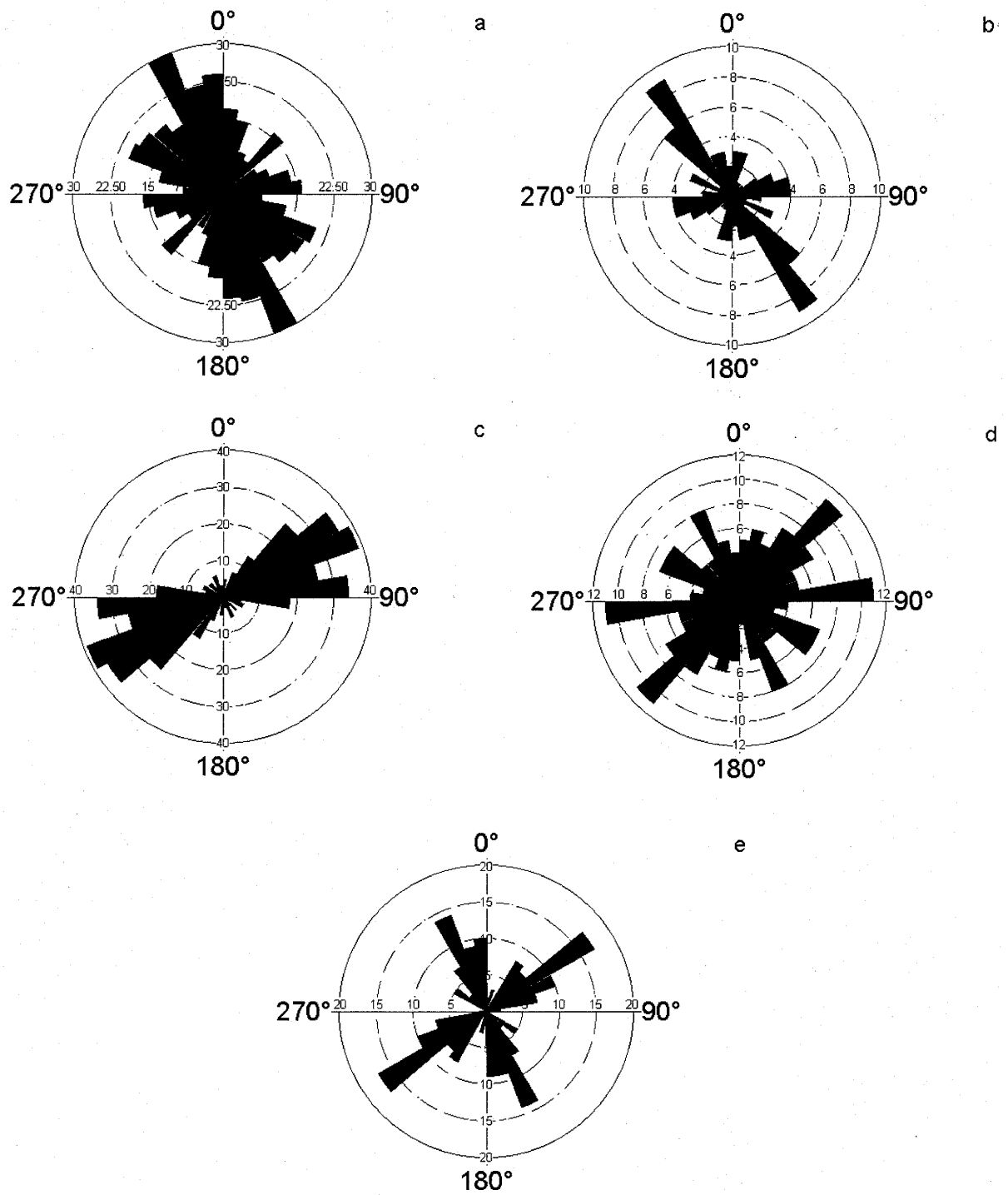


**Figure 14** Rose diagrams showing frequency of distribution of: a) sinkhole long axes orientation, b) Cutta Cutta Cave guiding fractures, c) lineaments from the geological map, d) Tindall Cave guiding fracture, e) lineament from the topographical map

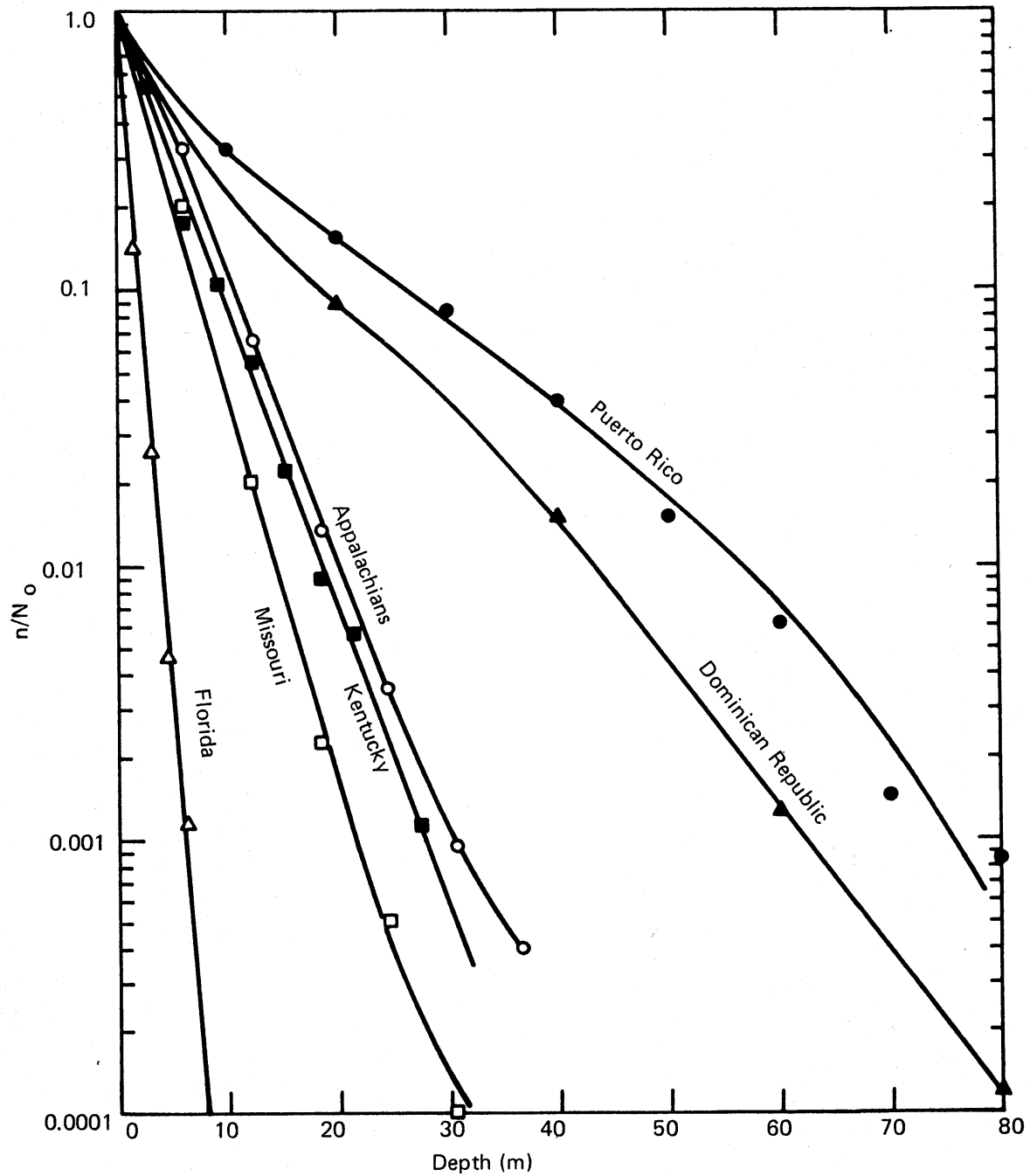


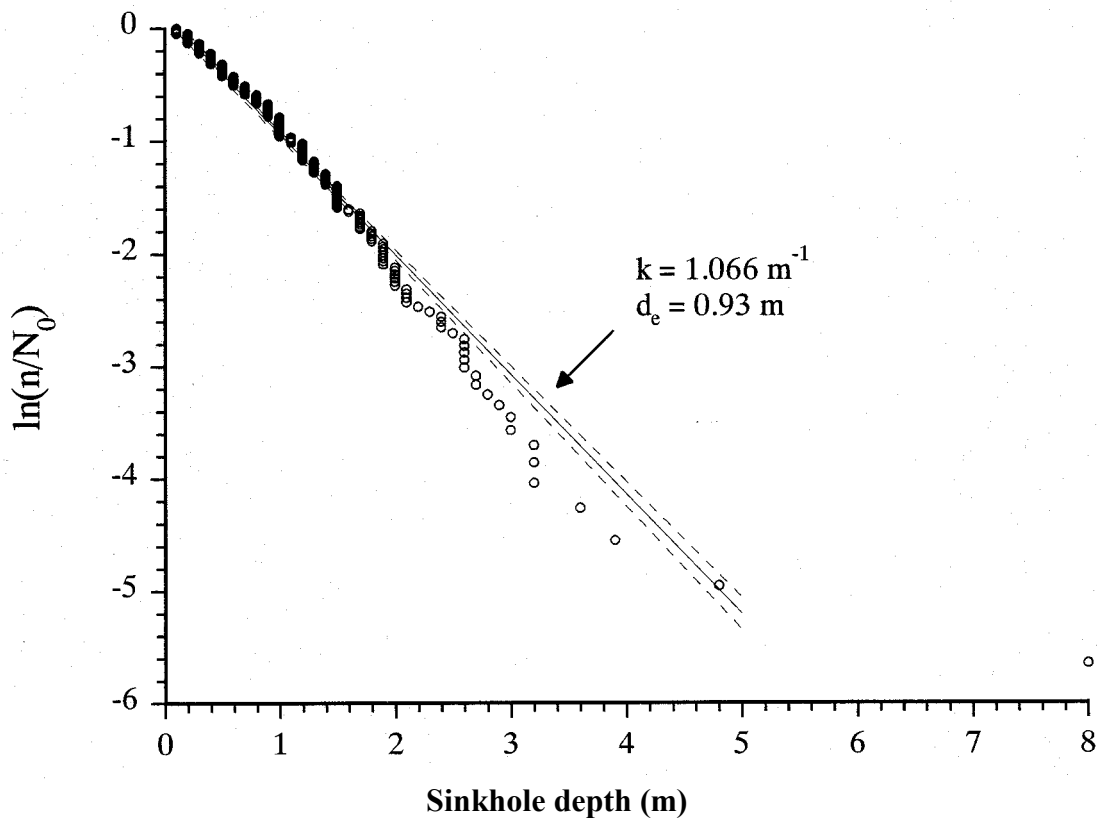
**Figure 15** Sinkhole frequency-depth distributions for six karst regions. These data were fitted to the equation  $n = N_0 e^{-kd}$  to obtain the fitting coefficients listed in Table 1

According to eqn (3), a population of sinkholes may be ranked by depth and the rank of each individual sinkhole divided by the rank of the deepest (Rank 1). When this parameter is plotted on a semi-logarithmic scale as a function of sinkhole depth, the graph will display a straight line if the distribution is exponential. Many karsts around the world, including the Tindall karst, display exponentially distributed sinkhole depths as shown in Table 1.

**Table 1 Sinkhole depth distributions in various regions**

Type of karst	Region	Density (sinks/km <sup>-2</sup> )	d <sub>e</sub> (m)	k (m <sup>-1</sup> )
Subarctic Karst	North Norway	-	1.37	0.727
Temperate Karst	Appalachians	1.25	4.48	0.22
	Kentucky	5.41	4.02	0.25
	Missouri	-	3.23	0.31
	Florida	7.94	0.85	1.18
Tropical Karst	Puerto Rico	5.39	11.35	0.088
	Dominican Republic	5.71	8.93	0.11
	Tindall Karst	0.57	0.94	1.066

The parameter  $d_e = 1/k$  is the characteristic depth of the sinkhole population and it reflects the internal relief in a given karst area. Several of the sinkhole populations in Appendix B are shown in Figure 16. The Tindall karst sinkhole population is different to most other samples, except for the Florida karst, with which it has a striking similarity. The interpretation of this is that both Florida and Tindall are low-relief karsts in which sinkhole development is dominated by formation of the shallow, suffosion type.

**Figure 16** Depth-rank relationship for 283 sinkholes in the Tindall karst

Sinkhole measurements were used to calculate the area of sinkholes. Subsequent to this they were classified into 5 size classes and plotted on the Map shown as Figure 17. There is little evidence in this map of clustering of particular sizes in particular areas other than a slight bias in the largest sinkholes toward the south-west of the study area. The complete set of morphometric analysis results for all sinkholes is presented in Appendix B.

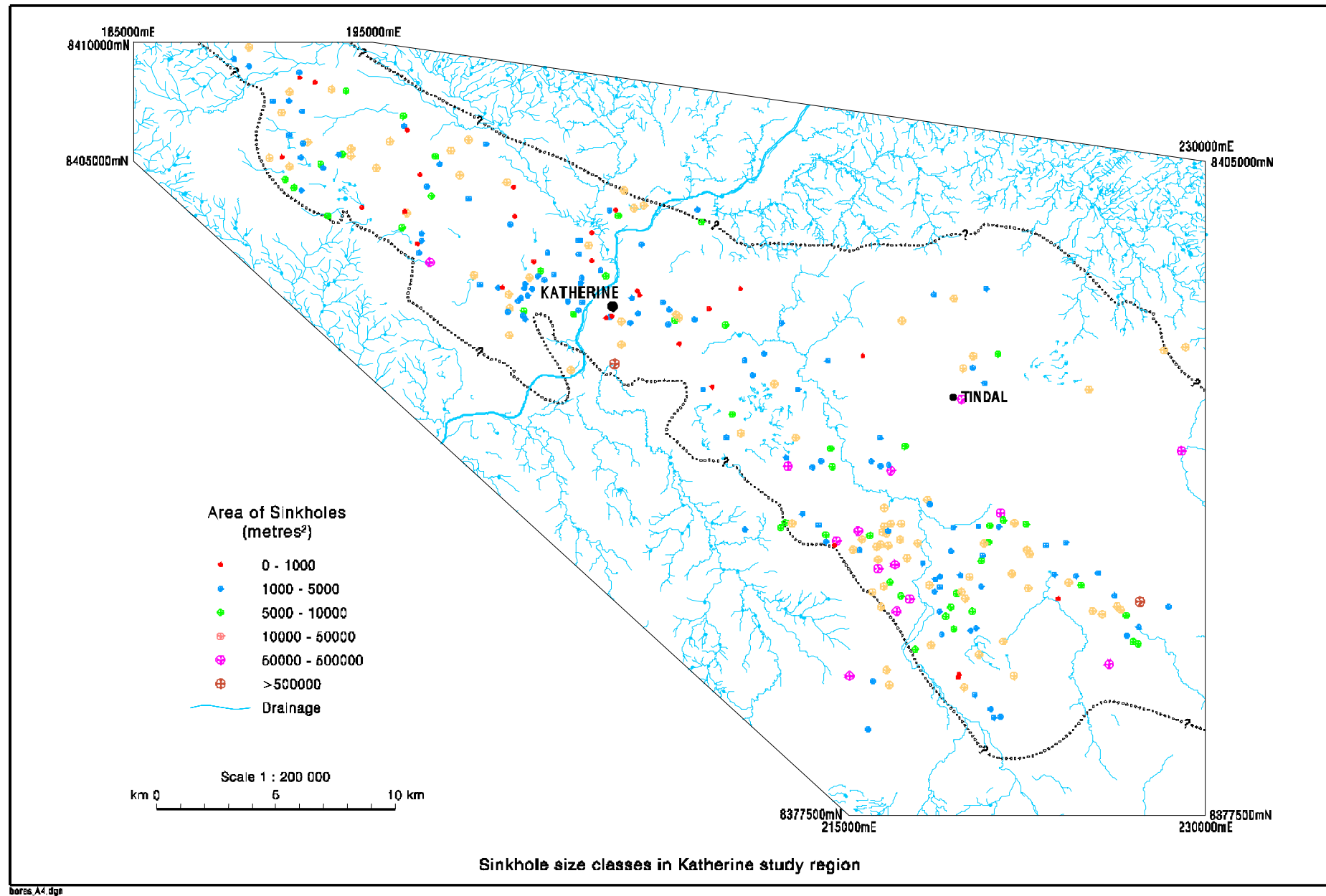


**Figure 17** Map of sinkhole size classes in Katherine study region

### **3.4 Lithologic controls on sinkhole development**

It is clear from the study that sinkhole density in the Katherine region is strongly related to lithology. The attached map 'Sinkholes in the Katherine Region' shows that only 1.5% of all sinkholes were located outside the Tindall Limestone.

Analysis of sinkhole distribution in the greater Daly Basin shows that only the Tindall Limestone and the Oolloo Dolostone are prone to significant sinkhole collapses. The Jinduckin Formation can not develop karst landscapes due to its lack of thick carbonate beds. The lithology of the Tindall Limestone is presented in Figure 18.

Examination of cuttings from drilled water bores shows a correlation between lithology and frequencies of cavity and sinkhole occurrence. Additionally, caves in Kintore Nature Park are developed in limestone and correlate with unit L1 and L2 of drill core hole CCVH No1 (Figure 18). Small cave systems developed in hills north of Zimin Drive can be correlated with unit L1 and L2. The main springs tapping the Tindall Limestone are developed in the lower part of unit L2.

Katherine sinkholes are more frequent in the areas where the cover is thin with 97.3% of all sinkholes located in zones where the overburden thickness is between 0-10m (Figure 19).

GEOLOGICAL LOG OF DRILL HOLE CCVH No. 1 INTERVAL 227m - 404m	DEPTH (m)	LOG	CORE RE- COVERY %
LIMESTONE, light grey, fine crystalline, fine vugs (<1mm diam.), abundant patches cream, coarse crystalline, coarser vugs (av. diam. 7mm), highly porous and permeable, calcite ? shell fragments at 233.16m; fractured at 230.45m at 25° to core axis.	227.85	L1	70.5%
LIMESTONE, light grey with patches of brown, abundant stylolites, scattered nearly vertical fractures, more massive rock than above.	261.33	L2	95.9%
MUDSTONE, dark grey, scattered ? shell fragments pyritic in part.	261.55 282.90	M1	100%
LIMESTONE, as interval 261.33 - 281.55m, trilobite sections (unverified) 1 - 2cm dimensions at 291.55m; breccia at 292.15m, interbedded brown, porous near base of interval, discoid vugs probably after gypsum.	281.55 282.90	L3	100%
MUDSTONE, grey grading red	295.47	M2	94.4%
MUDSTONE, dark grey; interbeds 2 - 70cm thick LIMESTONE, brown, very finely crystalline, finely vuggy.	299.41 303.60	M2	94.4%
LIMESTONE, cream, grading brown at 318.90m, very finely crystalline, similar to cream limestone above, scattered vugs 2 - 4cm diameter.	318.90	L4	78.3%
LIMESTONE, brown, medium crystalline, vugs, from fine in brown, to coarser (av. diam. 1mm) in cream, highly porous and permeable.	331.50	L5	93%
LIMESTONE, interbedded light grey and cream, fine crystalline, stylolitic, solution enlarged fractures at 45 - 60° to core axis, lined with calcite crystals to 5mm.	340.45	L6	90%
LIMESTONE, light grey and light brown patches, 3 - 4cm vugs at 344m, coarse calcite crystals infilling scattered stylolites.	344.11 348.52	L7	97.9%
LIMESTONE, cream patched brown, stylolites abundant (1 - 2cm spacing), less broken and less vuggy than preceding interval except in interval 361.41 - 361.81m where vugs to 1cm diameter common.	361.41 361.81	L7	97.9%
MUDSTONE, dark grey, scattered white calcite crystals, minor black interbedded SHALE and cream LIMESTONE, brown, CHERT in interval 347.05 - 347.59m.	362.05 366.59	M3	98.6%
LIMESTONE, light brown patched light grey, contorted black laminae at <5mm intervals, vugs to 1cm diam. one interbed CHERT, in interval 366.59 - 366.76m, vertical solution enlarged fracture in interval 367.94 - 368.64m, wavy black SHALE interbeds to 1cm thick, interval 379.90 - 392.10m; scattered vugs to 1cm diam., 389.49 - 392.10m.	366.59 392.10	L8	98.1%
MUDSTONE, red, minor buff and grey limestone, and grey mudstone.	392.10		93.2%
BASALT, dark grey, red brown weathered basalt in top 5m of interval.	404.62		99%
NOTE : L1 THROUGH TO L8 ARE UNITS OF TINDALL LIMESTONE			

**Figure 18** Stratigraphy of the Tindall Limestone (Lau 1981). The sinkholes and caves are developed in unit L1 and L2

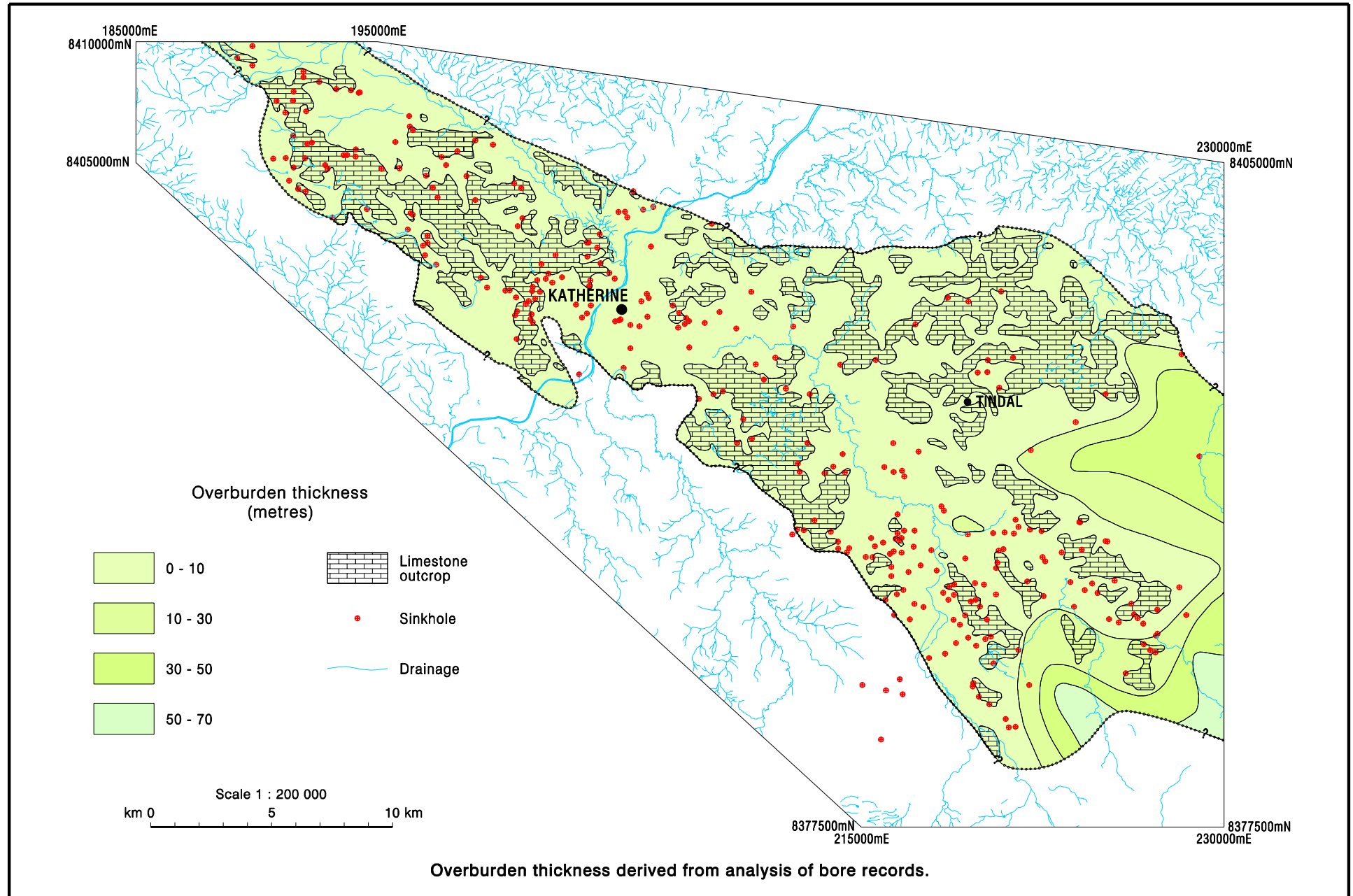


Figure 19 Relation between thickness of overburden and sinkhole distribution and location

### 3.5 Polje

North of Katherine town between Stuart Highway, Zimin Drive and Florina Road, lies a flat floored enclosed depression. This area is known locally as Lake Hickey. This terrain behaves as a base-level polje during flood periods. The polje floor is cut entirely across karst rock but is located in the epiphreatic zone and is consequently inundated at times when the water table is high (See Plate 14). A schematic, cross-sectional diagram of this area is shown in Figure 20.



**Plate 14** Polje in the Katherine region (Lake Hickey). Photograph taken on 14 March 2001 during a helicopter reconnaissance

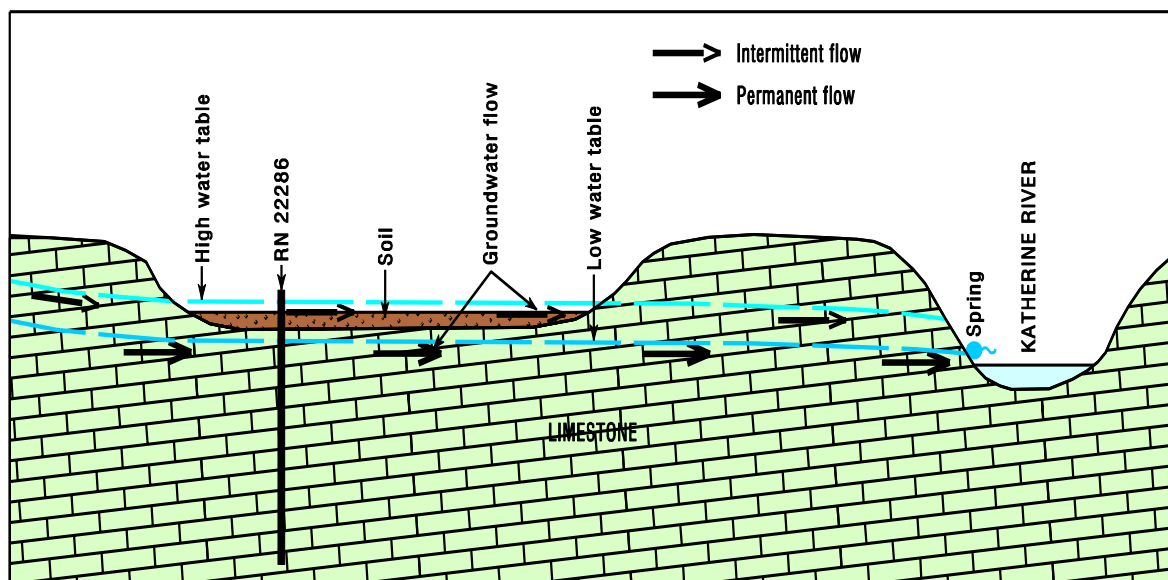


**Figure 20** Diagram of base-level polje at Lake Hickey. The low water table represents the dry season water table level while the high water table represents the wet season water table in Katherine. Water table fluctuations between the wet and dry seasons in the Lake Hickey polje region have been measured as high as 9.5m

Lake Hickey is inundated during periods when the water table is high. This has occurred several times during last 50 years and is reported in 1957/58 and 1982/1983 (Personal Communication from Katherine citizens) and during 1998, 1999, 2000, 2001 (data obtained from DIPE recorder). After the flood in January 1998 a data logger was installed on Bore RN 22288 located within the polje. Data analysis shows that in 1999 this terrain was under water for 49 days whereas in the year 2000 the water table was above the ground for 10 days.

Increased frequency and extent of flooding of polje terrain is connected with several factors. The most important is periodic rising of the water table. The groundwater table had steadily risen since the 1996 wet season due to three subsequent very high annual rainfalls. The average rainfall for Katherine is 966 mm (data from Katherine Post Office Station). In 1996, the total annual rainfall was 921 mm; in 1997, it was 1197mm; in 1998 it was 1493 mm; in 1999, it was 924.0 mm and in year 2000 it was 1275mm (data from R8140001 Katherine River at Railway Bridge). In January 2001, a monthly rainfall of 514mm raised the water table above the ground and Zimin Drive and Florina Road were inundated. Unfortunately due to this rise, the level recorder on Bore 22286 was flooded and data were lost. Nonetheless, surface water was visible in Lake Hickey until the end of June 2001.

After the floods in April 1998 and in February 2001, surveys of Lake Hickey were conducted by boat. During the latter survey, field analyses of temperature and dissolved oxygen were undertaken through the profile of Lake Hickey to estimate interactions between groundwater inputs and the surface water impounded in this polje region. Figure 21 shows the transect lines along which surface dissolved oxygen data was obtained. Contour diagrams of dissolved oxygen concentrations at the surface (0.1m) and at depth 2.5m are shown in Figure 21 and 22 respectively.

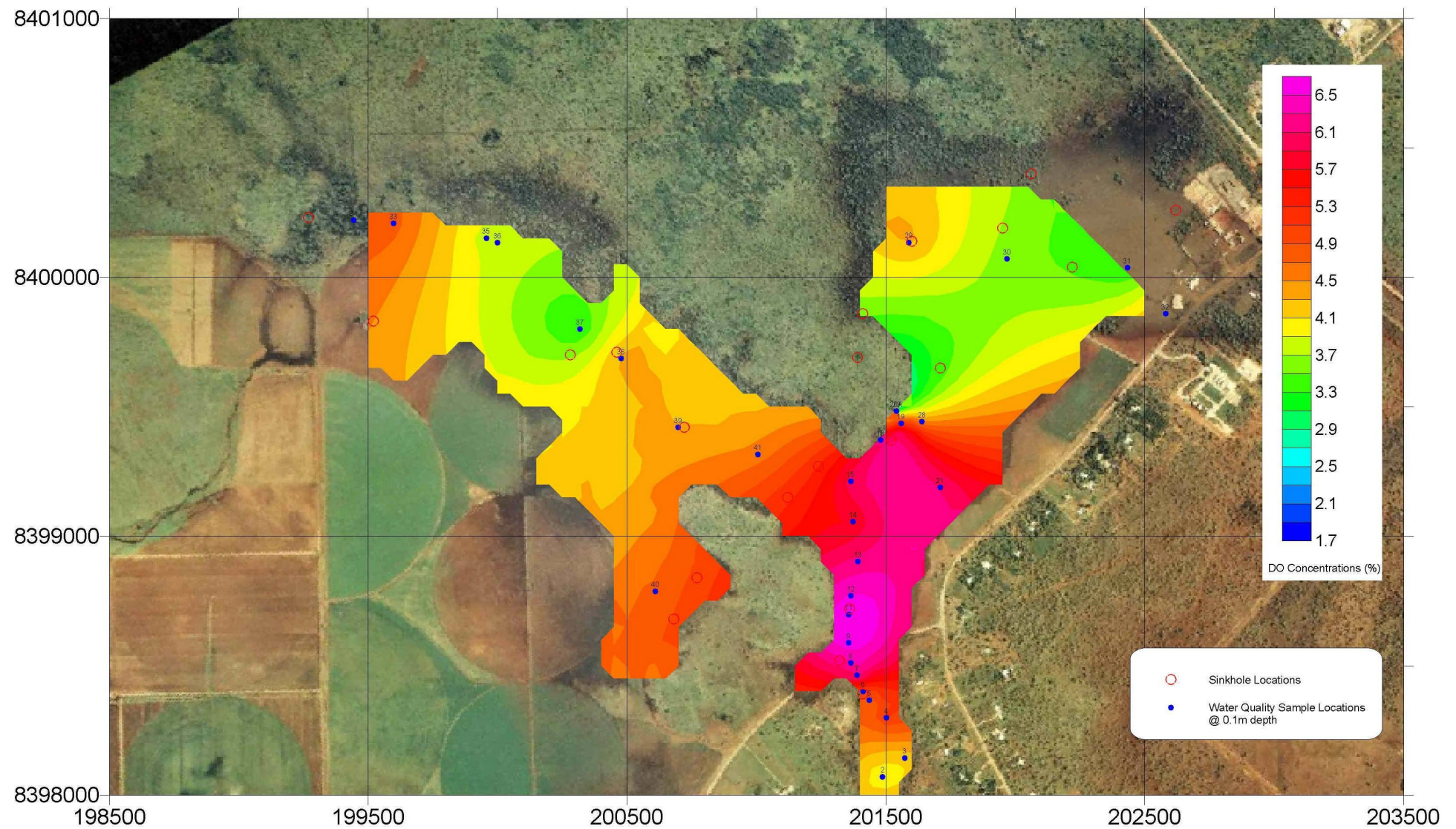


**Figure 21** Map of the sampling points along the two transects across the inundated polje (Lake Hickey) and Dissolved Oxygen concentration contours (13-14.02.2001) at depth 0.1m (surface)

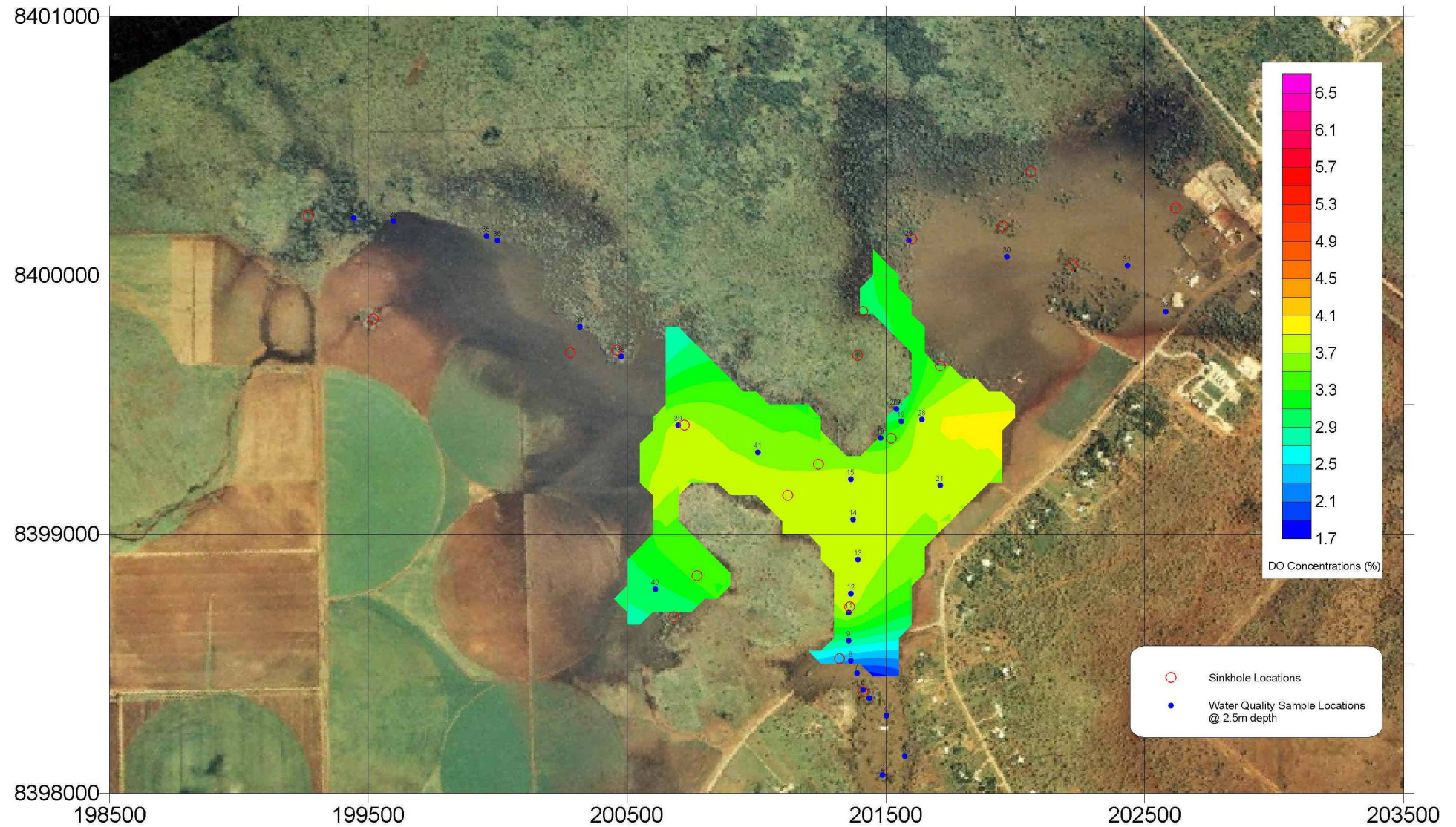


**Figure 22** Dissolved Oxygen concentration contours in Lake Hickey (13-14.02.01) at depth 2.5m

The maximum depth of Lake Hickey at the time of sampling was ~4 metres. Wind speed on the days of sampling was significant, ranging during the time of sampling from 1.2 to 12.6 km/hr. Thermal stratification was absent implying that the lake at this time would be hydraulically fully mixed (K.T. Boland, pers. comm.). Thus, the existence of water at depth with significantly lower dissolved oxygen concentrations indicates the inflow of groundwater (with low dissolved oxygen) into Lake Hickey. This can be observed in various regions around the lake (See Figures 21 and 22) and represents clear evidence of sites where groundwater is entering via subterranean sources.

### **3.6 Historical information about sinkholes in the study area**

Sinkhole formation in Tindall Limestone in Katherine Region was not monitored on a permanent basis. Thus, information about this phenomenon is scattered and incomplete. Anecdotal historical records were obtained from government workers (oral information) from the Department of Infrastructure, Planning and Environment formally the Department of Transport and Work, Roads Division and the Department of Land Planning and Environment. A history of sinkhole formations is tabled below.

**Table 2** Historical information about formation of sinkholes in the study area

<b>Date of sinkhole formation</b>	<b>Sinkhole location</b>	<b>Sinkhole description</b>
Late seventies		Part of Stuart Highway disappeared to sinkhole formed next to Cutta Cutta turn off
Early seventies	AMG co-ordinate 53L 224066-8390093	Group of sinkholes collapse; steep wall exposing limestone prongs and pipes filled with red soil
Since Stuart Highway Deviation near Tindal RAAF Base was constructed 1984 to 1994	AMG co-ordinate 53L 224045-8390113 AMG co-ordinate 53L 2240024-8390126	Several sinkholes along the Highway corridor were observed and infilled by pumped grout or concrete; between Ch.321km 120m and Ch.338km400m south of Darwin.
1993 after wet season	AMG co-ordinate 53L 227250-8385500	Collapse in red soil with steep wall (6m deep) formed in south-west corner of Cutta Cutta Nature Park; underlain siltstone and limestone exposed with cave entrance
1997 after wet season	AMG co-ordinate 53L 223868-83394254	Overnight collapse up to 9m in red soil, steep walls along the road to gold mine
1998	AMG co-ordinate 53L 224066-8390093	Group of sinkholes collapse; steep wall exposing limestone prongs and pipes filled with red soil along the Highway south of previously capped sinkholes
1998 after flood in January	AMG co-ordinate 53L 193333-8408014 AMG co-ordinate 53L 195901-8404767	New sinkholes were observed in Katherine Rural Collage collapse in red soil with steep wall, underlain limestone invisible
1999	AMG co-ordinate 53L 222012-8393100	Deep (6-10m) collapse along the service road next to Tindal RAAF Base; steep wall exposing limestone prongs and pipes filled between with red soil
1999	AMG co-ordinate 53L 225101-8389338	Deep (6-9m) opening was noted along the Stuart Highway 7 km northwest of turn to Cutta Cutta Nature Park. steep wall exposing limestone prongs and pipes filled between with red soil
2001 after wet season	AMG co-ordinate 53L 228152-8387430	Collapse (8m deep) was observed in south-east corner of Cutta Cutta Nature Park collapse in red soil with steep walls; siltstone and limestone underlain exposed and also opening to underlain cave system visible on the bottom;
2001 after wet season	AMG co-ordinate 53L 194215-8407886 AMG co-ordinate 53L 194262-8407906	Two sinkholes (3-5m deep) observed in paddock in Katherine Rural Collage north of Katherine; collapse in red soil with steep walls

### 3.7 Sinkhole locations

During the desktop study and subsequent field reconnaissance, 283 sinkholes were identified and assessed. These are shown in Figure 23.

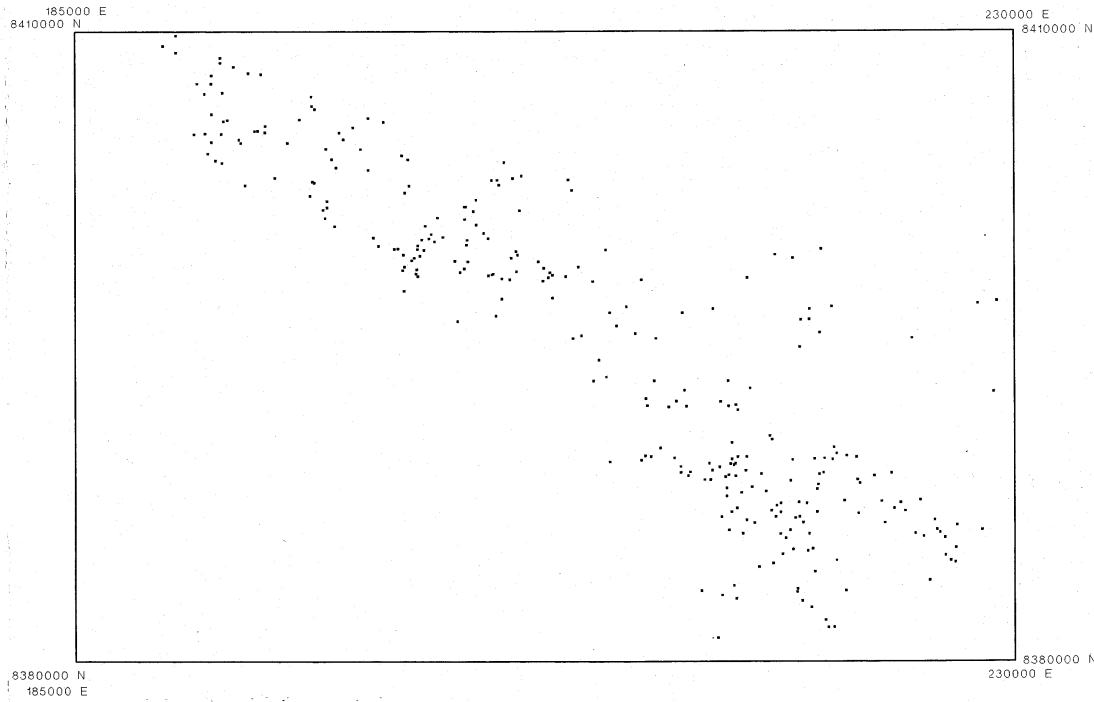


**Figure 23** Map showing sinkhole distribution in the study area

The sinkhole data base was combined with geological data sets and plotted as a map showing the relationships between sinkhole distribution and geology, depth to the bedrock, surface topography and morphology.

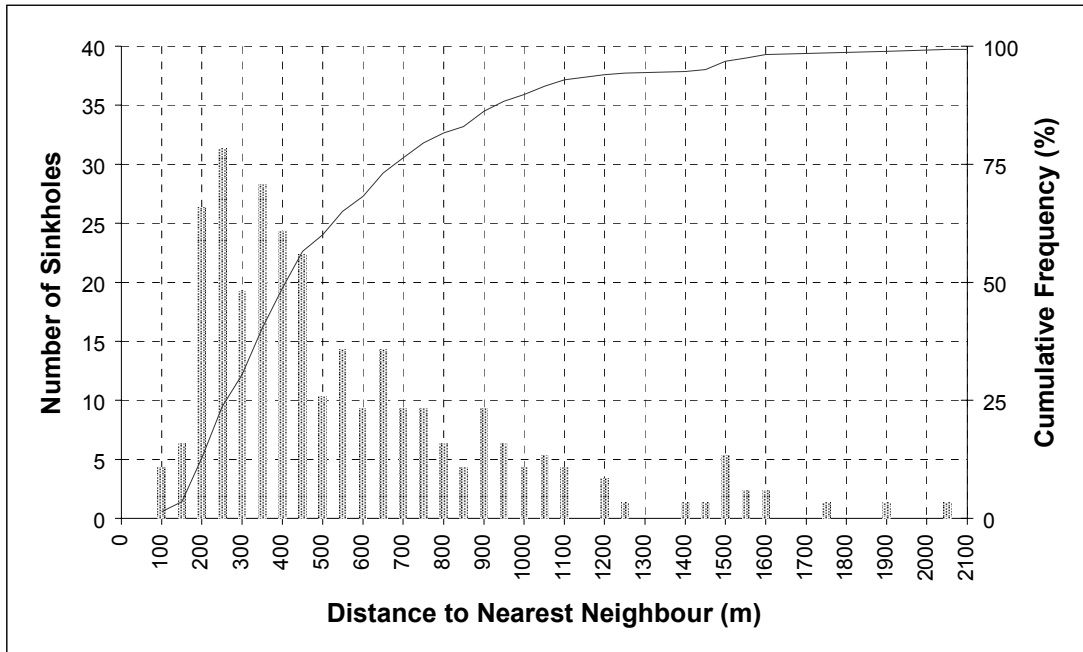
To analyse the distribution pattern of sinkholes, nearest-neighbour analysis was used. The sinkholes were categorised into one group of 283 sinkholes in the Tindall Limestone. All the sinkholes in the study area were selected for an extended nearest-neighbour analysis and compared with the Poisson distribution. “Nearest-neighbour analysis compares characteristics of the observed set of distances between pairs of closest points (sinkholes) with those that would be expected if the points (sinkholes) were randomly placed.” (Davis, 1981). The analysis results are shown in Figure 24 and Figure 25.

Figure 24 displays the histogram and cumulative fractions of the nearest-neighbour distances of the sinkholes. Figure 25 shows that the nearest-neighbour distance distribution is not significantly different from the Poisson distribution for sinkhole in the Tindall Limestone. The Poisson Process describes randomly distributed data. The ratio

$$R = \bar{d} / \bar{\delta}$$

(where,  $\bar{d}$  is the observed mean nearest-neighbour distance between points and,  $\bar{\delta}$  is the expected mean nearest-neighbour distance) represents the nearest-neighbour statistic and ranges from 0.0 for a distribution where all points coincide and separated by distances of zero to 1.0 for a random distribution of points. The calculated ratio from the study area value of

0.8 shows that sinkhole distribution in Tindall Limestone area of Katherine region is essentially random.



**Figure 24** Histogram and cumulative frequency of nearest-neighbour distances of sinkholes in Tindall Limestone. The mean distance = 539 m; median = 404 m; Stan.dev = 454 m

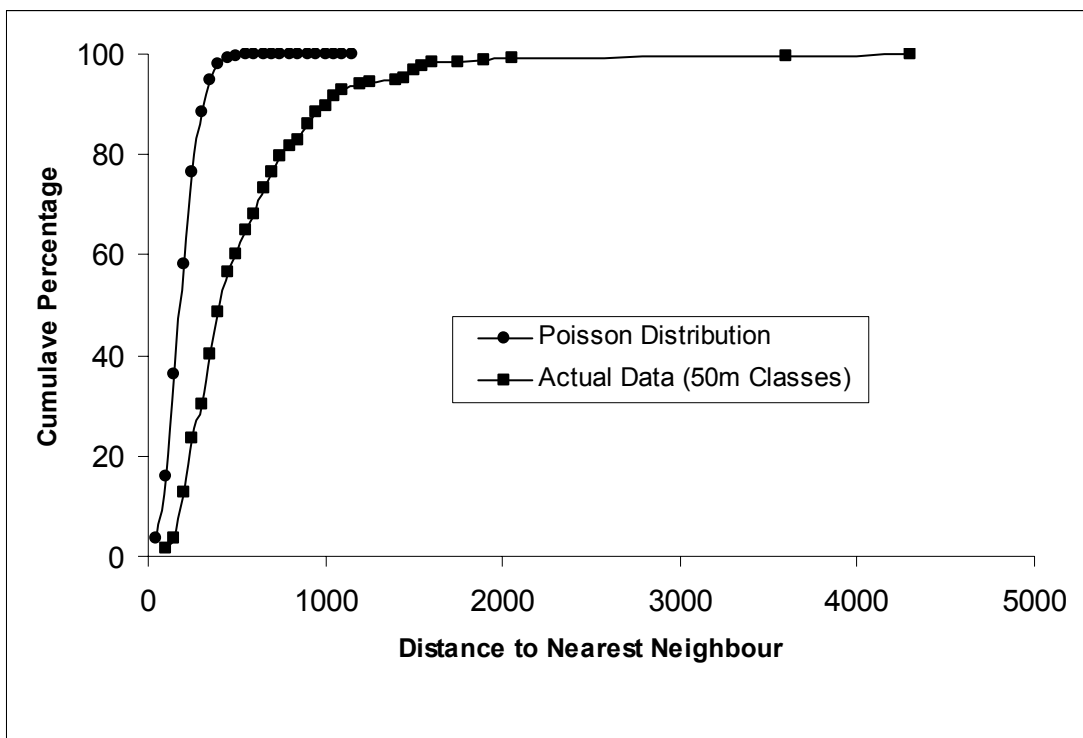


**Figure 25** Nearest neighbour and Poisson distribution of sinkholes in the study area.

### **3.8 Relationship between sinkhole development and topographic factors**

The study area of the Tindall Limestone is at elevations between 100 and 220m above sea level. Karst terrain is extensively developed on the limestone. Massive limestone ridges with well-developed towers, pinnacles, pavements and cave systems are present north of Katherine River and cover about 40% of this land mass. South of Katherine River, this terrain covers approximately 30% of that land area. Limestone outcrops are scattered on flat to gently undulating terrain covered by loamy red earths. Vegetation is dominated by low open woodland to mid-high woodland. Small creeks form broad drainage flats with seasonally ponded areas. These areas have very slight slopes that are rarely channelled to a significant degree. The major river in this terrain is the Katherine River. In its urban path, this river forms a deep valley cutting into the limestone formation. The river flows from NE to SW across the Tindall Limestone. In its central section (within the Daly Basin), it changes direction and flows NNE to the Timor Sea.

Analysis of their spatial distribution in relation to land form and soil units, shows that 78% of sinkholes lie in flat to gently undulating terrain. In this group 73% of sinkholes are located in terrain covered by red, loamy earth and 5% of this terrain is covered by yellow, loamy earths. 14% of sinkholes are located in hilly terrain with slopes ranging from 5-15%. Soils in this latter region are generally shallow or skeletal (Figure 26).

The sinkhole population is nearly equally distributed between elevation 100-120m (34.03%) and elevation 120-140m (37.54%). A further 23.16% lie between elevation 140-160m and the smallest group of 5.26% between elevation 160-180m. From this data, it would seem that the distribution of sinkholes is not controlled by elevation.

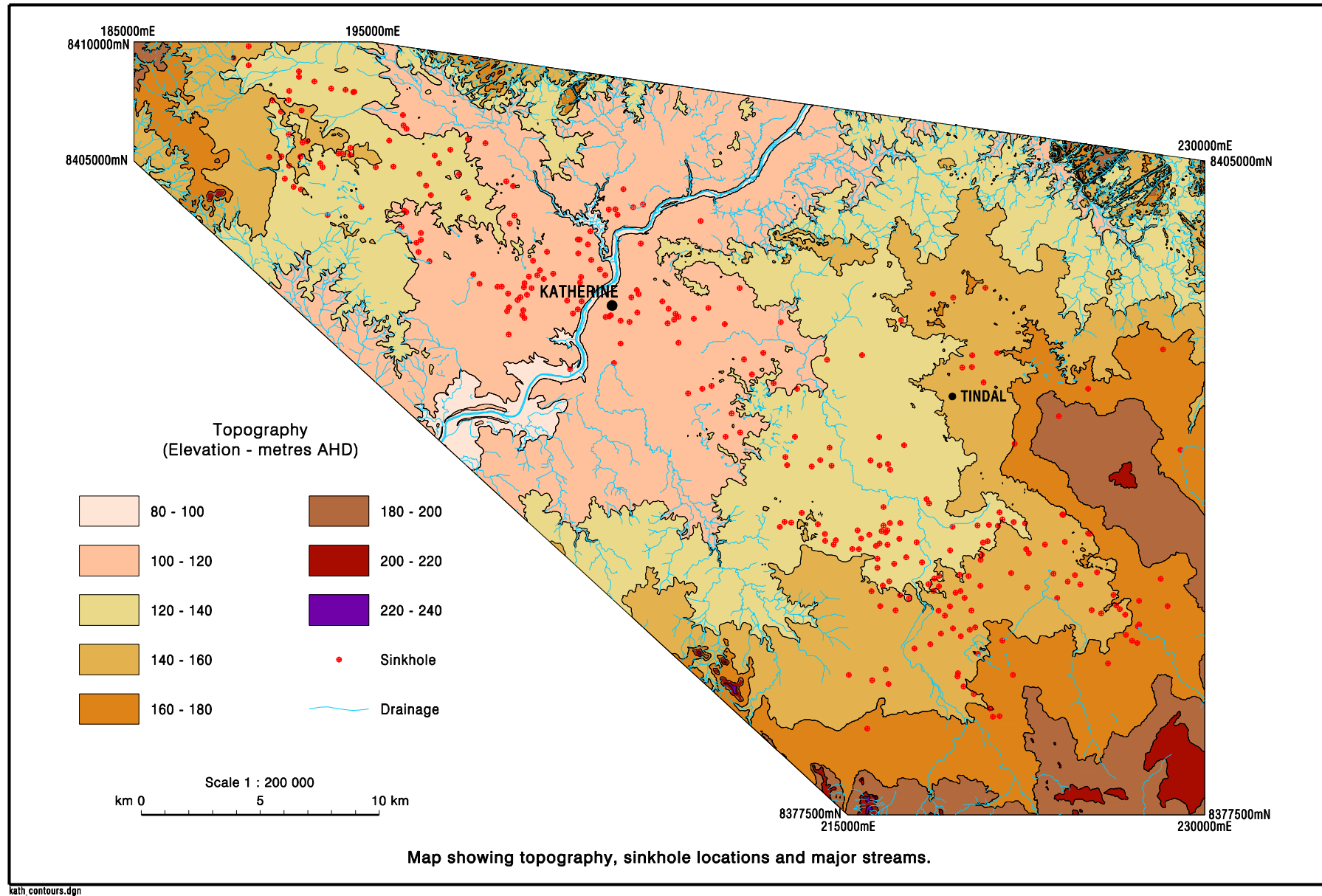


**Figure 26** Map showing sinkhole distribution in relation to elevation

### 3.9 Comparison of sinkhole development to depth to the water table.

Analysis of data obtained from water bores in the region, shows that the water table is emergent on and above the land surface at only one place in the study area. This is at the site of Lake Hickey, between Zimin Drive, Florina Road and the Stuart Highway. On the remaining terrain, the water table fluctuates between 25.45m (north of Katherine River) and 8.5m (south of Katherine River).

About 20 monitoring bores are located on the study area but only a few have continuous data loggers installed. Figure 27 shows plots of maximum (wet season) and minimum (dry season) levels recorded during this project. In Bore RN 32747, located in Kintore Nature Park, a minimum water level of 25.45m and a maximum of 9.39m below ground level were recorded. This data is however not complete, due to the loss of maximum readings that were out of data logger range. During the 2000-2001 year, a water table fluctuation of 16m was observed in this area. A data logger on Bore RN 22288 and located within the polje landform recorded a maximum fluctuation of 10.16m during 2000/01. Some data at this site were also lost because the recorder was inundated by water. The recorder located in Cutta Cutta Nature Park showed only an 8.5m change in water table over the same period. The water table of limestone aquifer in the study area is shown in Figure 27.

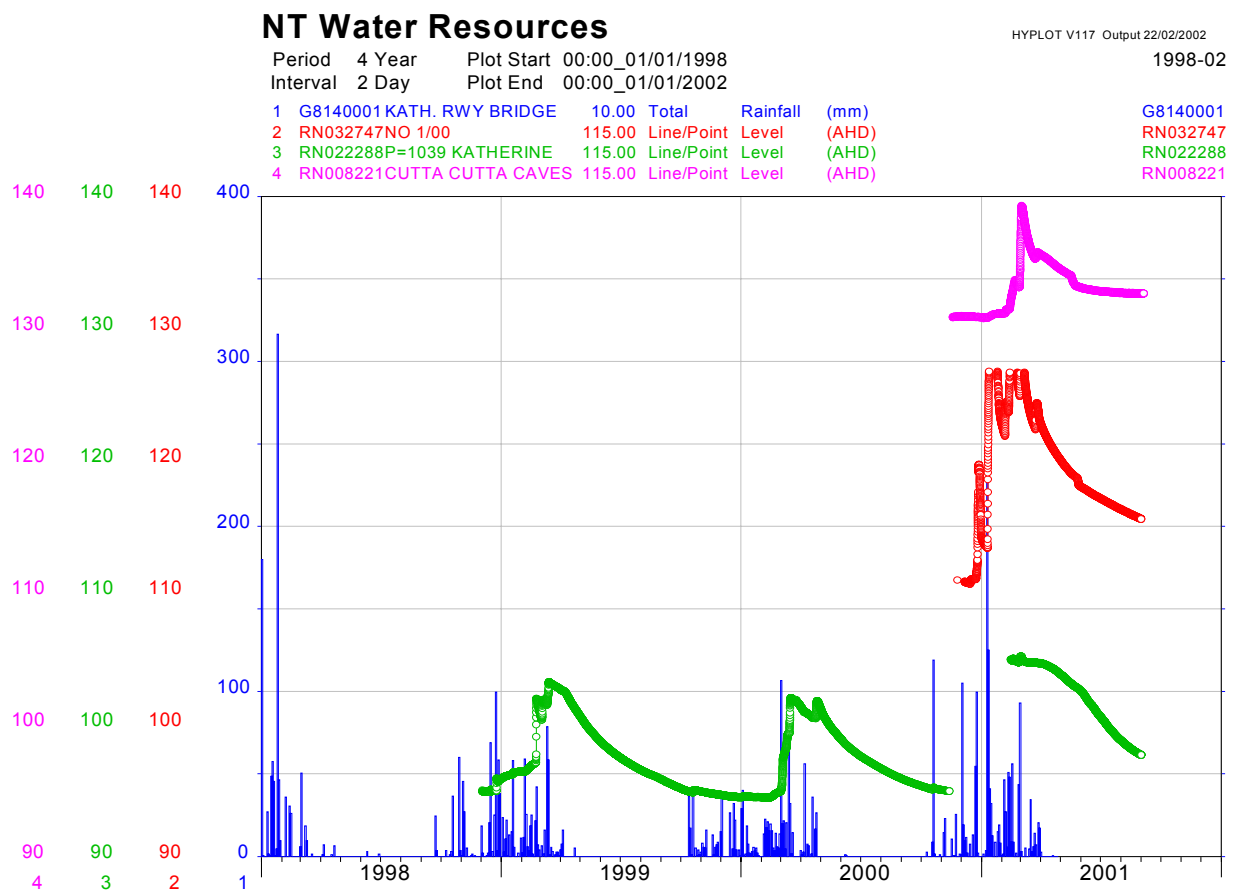
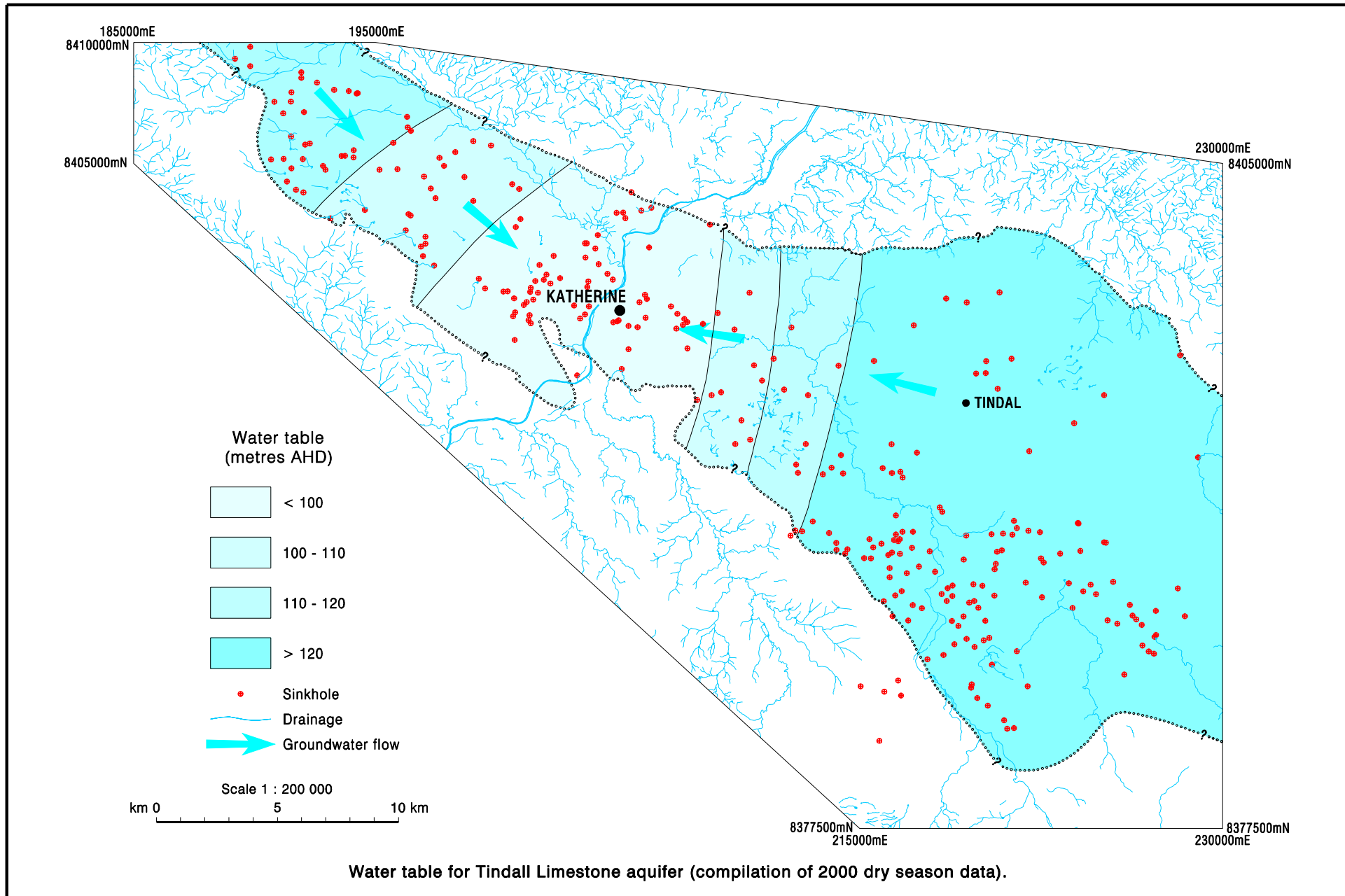


**Figure 27** Variation in groundwater level in Tindall Limestone in Katherine study area



kath\*SWL.dgn

Figure 28 Water table in limestone in the study area

## **4 Discussion**

### **4.1 Search for surface signatures of newly-forming sinkholes**

This project includes the first comprehensive description of sinkhole populations and their characteristics in Katherine region. Many sinkholes were formed prior to human settlement in the Katherine region. During the study period, a database of existing sinkholes was established. This assists the continued search for new sinkholes or new surface signatures of newly forming sinkholes. During field reconnaissance, fresh scarps on sinkholes near Cutta Cutta Nature Park demonstrate recent subsidence or collapse. Also new sinkhole collapses related to the ponding of rainwater were located in the grounds of Katherine Rural College.

New sinkholes were located from the air during the helicopter reconnaissance in 1994 and 2001. Based on this, it is clear that acquisition of aerial photographs repeated through time at a site of interest is an effective method to detect newly forming sinkholes. Many early surface changes not noticeable from the ground can be easily observed using aerial photography.

### **4.2 Water table fluctuations**

The density of sinkholes and their depths are often dependent on the depth to the water table. Sinkholes will sometimes develop more rapidly where the water table is near the surface and/or fluctuates substantially. Dissolution occurs most rapidly at the top of the water table due to mixing of waters of different carbon dioxide partial pressures and degrees of calcite saturation. Piping of sinkhole fills is enhanced where there is a significant change in the depth to the water table, be it natural or man-induced. Therefore, a water table (piezometric surface) map should be made for any area of concern and water levels in bores monitored.

Fluctuations in the water table in limestone are of two general categories, seasonal and pulse. Plots of water table height data for 1999-2001 show obvious seasonal fluctuations. In the polje area, pulse loadings from single storm events, or from a series of storms, were clearly observed. Locally, these events can trigger a rise in the water table as much as 1.8m in 24hours. This phenomenon was observed in the study area in January and February 2001.

Sinkholes play a dual role in karstic settings. Firstly, they act as a collecting basin for runoff. Secondly, surface water collected in the sinkhole depression, drains vertically through the regolith into bedrock fractures and downward to recharge the water table. Field observations 1999-2001 and satellite image analysis in March 1998 show that the sinkhole population can be classified into the following groups:

- a) sinkholes with rapid drainage within 24 hours
- b) sinkholes that drain slowly i.e. more than 24 hours
- c) sinkholes with an impervious bottom (hydraulic conductivity,  $k=0$ )

The satellite image from March 1998 shows several sinkholes (black oval spots) with impervious bottoms concentrated south of Tindal RAAF Base (Plate 15). These can hold water until late in the dry season. These types of sinkholes are important as permanent or semi-permanent wetland environments in the Katherine limestone.



**Plate 15** Sinkhole at AMG co-ordinate 53L 217570-8386610 located south of Tindal RAAF Base (photo taken 16 August 2000, dry season). It represents a sinkhole with an impervious bottom and may hold water throughout the year

During the wet season fieldwork, sinkholes with rapid drainage (Groups ‘a’ and ‘b’) were observed along the Stuart Highway. Remnant debris and silt on the edges of the sinkholes mark the maximum water level.

### 4.3 Sinkhole collapse causes.

Sinkhole collapses and their associated geological and hydrological causes have been studied in many places in the world. Many of these studies involve single collapse events that occurred concurrently with industrial subdivision/development, highway construction, sewage lagoon construction, mining and groundwater extraction. In the early 1980’s, an approach to these events was initiated in vulnerable areas in the United States. This involved the systematic examination of sinkhole collapses on a regional basis aimed at defining causal factors specific to that region. Regional studies of sinkholes collapses are needed before the dynamics of sinkholes collapse can be known in sufficient detail for accurate prediction, and before remedial techniques can be developed.

In this study, two sinkhole areas that have recently collapsed were monitoring closely. The first area is located along the fence on the southern part of Cutta Cutta Nature Park (AMG co-ordinate 53L 227250-8385500). The second area is located between the old North Australia Railway embankment and the Stuart Highway some 3.5km north-west of the turnoff to Cutta Cutta Nature Park (AMG co-ordinate 53L 225101-8389338). In both instances, collapse is related to changes in surface drainage. In the second cause deforestation of adjacent land (increase recharge) could also have roll in sinkhole collapse.

The collapse in the first sinkhole area (AMG co-ordinate 53L 227250-8385500) along the fence was observed by a ranger after the 1993 wet season. The sinkhole collapsed overnight to form a substantial depression. During a field visit in 1994 this sinkhole was measured (Report SE Lauritzen and D.Karp 1995) and its estimated volume calculated to be 700m<sup>3</sup>. Further measurements were conducted during this project to calculate the growth of this sinkhole. Over the 5 years 1994-1999, the sinkhole has become substantially larger in both lateral and horizontal dimensions and in 1999 openings to a subterranean cave system were exposed.

Surveys undertaken in 2000 and 2001 revealed that the sinkhole volume had increased in volume by 19.3% during this one-year period. Figure 28 shows the development of this sinkhole between 2000 and 2001. Table 3 shows a theoretical annual volume increase for this sinkhole assuming that the measured percentage increase (between 2000 and 2001), was similar to that since its initial formation in 1993.

**Table 3** Growth of the sinkhole located along the fence on the southern part of Cutta Cutta Nature Park, since formation in 1993

Year	Volume (m <sup>3</sup> )	Volume collapse (m <sup>3</sup> )	Volume %
2001	2870	***	***
2000	2405	465	19
1999	1940	375	19
1998	1565	303	19
1997	1262	244	19
1996	1018	197	19
1995	821	159	19
1994	663**	128	19
1993	*		

\* In 1993 this sinkhole formed overnight

\*\* In 1994 its volume was about 700m

\*\*\* 19.33% (assumed) growth every year starting from 1993 – 1994

The collapse in the second sinkhole area along the Stuart Highway, triggered by alteration of surface drainage, was observed at AMG co-ordinate 53L 225101-8389338. At this, site a group of six sinkholes (two large and four smaller ones) collapsed in the early 1970's where water was ponding each wet season between the highway and the railway line. Surface water stream flow was interrupted by highway and railway construction and ponding was caused by inadequate culvert construction. A group of six sinkholes developed in a shallow depression. The largest sinkhole was 13.5m in diameter and about 9 m deep with a very irregular horizontal shape (Twidale 1984).

During the 1994 field visit an additional four sinkholes were located in this area. Three of these were approximately 3m x 6m at the surface and 5m to 7 m deep, with another having surface dimensions of 4m x 2m and 1m deep. These developed in 1993. In 1999, a new collapse 3.5m x 6.5 m and 7.3 m deep was found some 50m east of the existing collapses towards the Stuart Highway. The largest sinkhole of this group has changed little since its first observation by Twidale (1984). Field observations show that after sinkholes collapse, soil from the adjacent areas is washed into the sinkhole depressions exposing the surrounding bedrock surface (Figure 7).

Figure 29 Diagram showing evolution of a sinkhole AMG co-ordinate 53 L 22725008385500. Growth is calculated in Table 3

During highway construction (1984), more sinkholes similar to these described first by Twidale (1984) were developed (north from this location at AMG co-ordinate 53L 224074-8390091) and were closed by rock fill plugs and cement plates due their proximity to the highway. This type of remedy is inadequate as demonstrated by potentially serious wash-out around the filling medium, observed as far back as 1994. Successful construction (highways or other) in areas with these types of collapses requires more information and observation to properly understand the causal factors associated with sinkhole formation.

#### **4.4 Determine the effect of man's activities on sinkhole development.**

There is a clear need to distinguish between sinkhole development in a geological time scale and in a historical time scale. In a geological time scale, dissolution rates may increase the probability of collapse. In this case, the formation of sinkholes will be relatively slow. In historical time, the trigger mechanisms for sinkhole collapse (i.e. the sudden movement of soil) into a karst void beneath the surface may be rapid.

The study of sinkholes in the Tindall Limestone shows that present sinkhole collapses are often induced or accelerated by human activities. Triggering mechanisms include:

- water ponding due to road and subdivision construction
- modifications of surface runoff regime due to highway and railway construction
- leaky water and sewer lines
- major floods (e.g. 1998)
- land clearing for agriculture

A group of sinkholes developed in 1972 between the Stuart Highway and the old railway due to water ponding. These collapses were probably accelerated also by blasting undertaken during the construction of Tindal RAAF Base. Similar collapses occurred along the road to the Maud Creek gold mine after the 1998 flood. These were very likely due to modifications of the surface runoff regime.

New sinkhole collapses were noted in the grounds of the Katherine Rural College after the 1998 floods and the intense wet season in 1999/2000. Sinkhole development after floods may be considered as a natural phenomenon. In many cases however, human activity exacerbates this because of interference with major stream-flow regimes and deforestation. During the land units mapping in 1972 only 10 were located and are show on map "Katherine experimental Farm Land unit map". During this project field mapping 20 more sinkholes were discovered. The increase in sinkhole population is connected with human activity. It is important to monitor this terrain for future studies of sinkholes collapses.

## **5 Conclusions**

### **5.1 General**

Sinkhole formation in the Katherine region is a natural feature of the karst terrain associated with the Tindall Limestone. Human activities in some areas however, have increased the rate of sinkhole

formation and pose potential risks. These activities include road and railway and other construction activities that change the natural, surface flow regime and result in ponding of water in areas where sinkhole formation is probable. Risks include potential property damage due to collapse or subsidence but also more subtle issues such as groundwater contamination and flooding associated with inappropriate closure of sinkholes.

## 5.2 Further investigations

Further systematic studies of sinkhole formation in the Katherine region should be undertaken including detailed investigation of triggering mechanisms. These studies should be strategically designed to achieve the following objectives;

- To control and advise land users on the land degradation of limestone terrain in the Daly Basin. Data should be easy available to professional people, government departments and the public.
- To help land use planning in karst regions. This should include a series of maps outlining areas with subsidence susceptibility.
- To better understand and control development over the Tindall Limestone. In this aspect, further observations and studies should be established in the area surrounding the trench being constructed to drain water from the polje area known as 'Lake Hickey'. Excavation of soil in the trench corridor started in November/December 2001. This area, between Florina Rd, Zimin Dr and Katherine River, could supply important information for future construction proposed in the broader Daly Basin and the immediate Katherine region.
- To supply information about the behaviour of the Tindall Limestone aquifer and the function of sinkholes as recharge points. Data from monitoring points on sinkholes and water bores were established on the Research Station (DIPE) south of Katherine. These observation sites should be continued and data should be analysed and interpreted when sufficient is collected.
- To monitor sinkhole collapses and sinkhole development in Cutta Cutta Nature Park as a continuing program. This area is unique in the Katherine region because the times of initial sinkhole collapses are known. As a result, further observation will supply important information about sinkhole genesis and behaviour in the Tindall Limestone. The survey of sinkholes started in 1999 dry season.
- To continue monitoring of sinkhole collapses in the paddocks of the Katherine Rural College. Some data is available as far back as 1972. In particular studies should broadly focus on the influence of agriculture on limestone covered by soil and specifically:
  - sinkhole collapses
  - aquifer behaviour
  - soil erosion
  - land clearing for agriculture

### **5.3 Remedial protective measures for sinkholes**

A protection zone (100 m diameter?) should be established around sinkholes. Sinkholes behave as stream sinks and can carry pollutant directly to aquifers. Thus, surface runoff in town and along the Stuart Highway should not be directed to sinkholes. Such 'buffer zones' are similar in principle to the separation of septic systems and water extraction bores already subject to legislative requirements in the NT. Clearly also, sinkholes should never be used for rubbish disposal due to possible aquifer pollution.

Changes in local surface drainage due to construction etc. should be carefully considered and investigated in their context as possible sinkhole-collapse triggers. This will require detailed study in some cases to avoid situations that are already obvious e.g. sinkhole collapses along the Stuart Highway and railway.

Sinkhole should not to be filled with soil or closed unless necessary. They are natural connection points between surface drainage and groundwater and are important recharge conduits. Additionally, closing too many sinkholes in karst terrain can increase the probability of flooding.

Stormwater drainage should be diverted away from sinkhole openings because water flowing into the sinkholes may erode pre-existing cavities and cause more ground collapse. Additionally, stormwater drainage may contaminate the aquifer.

## **6 Acknowledgments**

Special appreciation is expressed to the late Dr. Jim Quinlan whose generosity and wise advice assisted the early genesis of this project. Professor Derek Ford also assisted in technical assessment of many aspects of the approach. Professor Stein Erik Lauritzen has been a consistent supporter of the project and committed much time and effort both in the fieldwork component and in technical discussions with many relevant parties. Finally to all of my colleagues in Natural Resources, I express my gratitude for their assistance to and at times, tolerance of me over the course of the project.

## 7 References

- Beck, B. F. (1984). A computer based inventory of recorded, recent sinkholes in Florida; Florida Sinkhole Research Inst, (U.of CentralFl., Orlando, Fl.) Report 84-1, 12.
- Davis, J.C. (1973). *Statistics and Data Analysis in Geology*, 2<sup>nd</sup> ed. John Wiley & Sons, NY.
- Doerfliger, N, Jeannin, Y, Zwahlen, F (1999). Water vulnerability assessment in karst environments: a new method of defining protection areas using a multi-attribute approach and GIS tools (EPIK method). *Environmental Geology* 39 (2) 165-176.
- Jennings, J.N. (1971). *Karst*: Cambridge, Mass., M.I.T. Press,
- Ford, D.C. and Williams, P.W. (1992). *Karst Geomorphology and Hydrology*, Chapman &Hall.
- Gams, I. (1978). The polje: the problem of its definition. *Z. Geomorph.* **22**, 170-181.
- Knapton,A., Geophysics of karst terrains. *Report 12/2002. Assessment Branch, Department of Infrastructure, Planning and Environment.*
- Kruse, P.D., Sweet, I.P., Stuart-Smith, P.G., Wygralak, A.S., Pieters, P.E. and Crick, I.H. (1994). Katherine, Northern Territory-1:250 000 geological map series. *Northern Territory Geological Survey Explanatory Notes* SD 53-9
- Lau,J.E., (1981) Daly River Basin data record. *Northern Territory Geological Survey, Technical Report* GS 81/29 (unpublished).
- Lauritzen,S.E., Karp,D., (1993). Speleological assessment of karst aquifers developed within the Tindall Limestone Katherine, Northern Territory. *Report 63/1993. Water Resources Division, Power and Water Authority.*
- Williams, P.W.(1971). Illustrating morphometric analysis of karst with examples from New Guinea. *Z.Geomorph.* **15**, 40 –61.
- Williams, P.W.(1972b). The analysis of spatial characteristics of karst terrains. In *Spatial analysis in geomorphology*, R.J. Chorley (ed.) 136-63 , London:Methuen.

## 8 Glossary

**Anisotropic.** The property of aquifer systems displaying different hydrological properties in different directions.

**Aquifer, karst.** An aquifer in which the flow of water is, or can be, appreciable through one more of the following: joints, faults, bedding-plane partings, and cavities – any or all of which have been enlarged by dissolution.

**Bedding.** Applies to rocks resulting from consolidation of sediments and exhibiting surfaces of separation (bedding planes) between layers of the same or different materials (e.g., shale, sandstone, limestone, etc).

**Bedding plane.** A plane that separates two strata of differing characteristics. Bedding planes play a crucial role in the inception and ongoing development of most caves and many surface karst features.

**Bedrock.** Solid rock underlying unconsolidated material.

**Carbonate.** A rock consisting mainly of carbonate minerals, such as limestone or dolomite.

**Carbonate rock.** A rock that consists of one or more carbonate minerals. Carbonate rock successions (or sequences) are those in which carbonate rock is dominant, but which also contain rocks of other lithology.

**Cave.** A natural opening formed in the rocks below the surface of the ground large enough for a man to enter. It may consist of single connected opening or series of small or large chambers connected by galleries. A cave is commonly formed in limestone by solution.

**Clint.** Slabs of limestone, parallel to the bedding, forming a pavement. Widened joints, or grikes, isolate individual clints.

**Conduit; karst conduit.** Relatively large dissolutional voids, including enlarged fissures and tubular tunnels: in some usage the term is restricted to voids that are water-filled.

**Conduit flow; karst conduit flow.** Underground water flow within conduits. Conduit flow is generally turbulent, but can also be laminar.

**Diffuse circulation; diffuse flow.** Circulation of ground water in karst aquifers (or other aquifers) under conditions in which all, or almost all, openings (primary and secondary) in the karstified rock intercommunicate and are full of water but have not been selectively enlarged in specific zones by dissolution, and so thus no concentration of ground water occurs in restricted conduits. The ground water flow is generally slow-moving, may be laminar, and have a uniform discharge and slow response to storms.

**Dissolution.** See solution.

**Dissolution of limestone.** The solubility of calcite (and hence of limestone) in pure water is very slow, but is vastly increased in the presence of carbon dioxide. This gas, dissolved in the water to produce carbonic acid, permits dissociation of calcium carbonate, and dissolution rates and loads

are therefore directly related to carbon dioxide content. This accounts for the importance to limestone dissolution of plant growth; soil water contains greatly more carbon dioxide than stream water.

**Epikarst; epikarst zone.** A relatively thick (the thickness may vary significantly, but 15 to 30 meters thick is a good generalisation) portion of bedrock that extends from the base of soil zone and is characterised by extreme fracturing and enhanced solution. It is separated from the phreatic zone by an inactive, relatively waterless interval of bedrock that is locally breached by vadose percolation. Significant water storage and transport are known to occur in this zone. Synonym: subcutaneous zone.

**Epiphreatic or intermittently saturated zone.** That is inundated seasonally or in storms by fast-flowing (and chemically aggressive) flood waters.

**Grike.** A solutionally enlarged vertical or steeply inclined joint in the surface of karst-land, extending for up to a few meters into the limestone. Grikes separate clints from one another.

**Impervious.** Not permitting the flow of water.

**Joint.** A break of geological origin in the continuity of a body of rock occurring either singly, or more frequently in a set or system, but not attended by a visible movement parallel to the surface of the discontinuity.

**Karren.** Channels or furrows, caused by solution on massive bare limestone surfaces; they vary in depth from a few millimetres to more than a meter and are separated by ridges. In modern usage, the terms are general, describing the total complex of superficial solution forms found on compact pure limestone.

**Karst.** A terrain, generally underlain by limestone or dolomite, in which the topography is chiefly formed by the dissolving of rock, and which may be characterised by sinkholes, sinking streams, closed depressions, subterranean drainage, and caves. The term karst unites specific morphological and hydrological features in soluble (mostly carbonate) rocks. Morphological features include karren, sinkholes (dolinas), jamas, ponors, uvalas, poljes, caves etc. Hydrological features include basins of closed drainage, lost rivers, estavelles, submarine springs, more or less individualised underground streams and incongruity of surface and underground divides.

**Limestone.** Sedimentary rock containing at least 50% calcium carbonate by weight. The purer limestones consist almost entirely of calcite.

**Pavement, limestone.** A bare plane surface of limestone, parallel to the bedding, commonly divided into blocks (clints) by solutionally widened joints (grikes) and pitted by solution pans.

**Pinnacle karst.** Tropical karst characterised by vertical rock blades fretted sharper by dissolution.

**Phreatic water.** That part of the underground water in karst limestone which lies within the zone of permanently saturated rock-the phreatic zone.

**Rillenkarren.** Solution flutes that occur only in places where fresh unspent precipitation is active and end where the water attains too high a content of lime or where water is added. Their length increases with slope, temperature, and rainfall: eventually reaching 1 m and more in tropics. Their width extends from 1 to 3 cm. They lie together in rows with no space between, with sharp intermediary ridges of no more than 1 cm in height.

**Saturated zone.** That part of the earth's crust beneath the regional water table in which all voids, large and small, are ideally filled with water under pressure greater than atmospheric. Synonym: phreatic zone.

**Sinkhole; doline.** A general term for closed depressions. They may be basin- or funnel-shaped hollow in limestone, ranging in diameter from a few meters up to a kilometer and in depth from a few to several hundred meters. Some sinkholes are gentle grassy hollows; others are rocky cliff-bounded basins. A distinction may be made by direct solution of the limestone surface zone, (solution sinkholes), and those formed by collapse over a cave, (collapse sinkholes) but it is generally not possible to establish origin of individual examples.

**Solution.** A process of chemical weathering by which rock material passes into solution: e.g. the dissolution and removal of calcium carbonate in limestone by carbonic acid derived from rainwater containing carbon dioxide acquired during its passage through the atmosphere.

**Tower karst.** Karst topography, common in the tropics, characterised by isolated residual limestone hills displaying numerous shapes separated by areas of alluvium.

**Unsaturated zone.** The zone between the land surface and the water table. Synonym: vadose zone.



## **Appendix A**

### **Water Quality Data for Springs**



# Northern Bank Spring G8145358

SPRING REGISTERED NUMBER	DATE OF SAMPLING	pH	ELECTRICAL CONDUCTIVITY ( $\mu$ S at 25° C) Field/Lab	TOTAL DISSOLVED SOLIDS (mg/l by evaporation at 180° C)	SODIUM, Na	POTASSIUM, K	CALCIUM, Ca	MAGNESIUM, Mg	IRON (TOTAL), Fe	TOTAL HARDNESS (as CaCO3)	TOTAL ALKALINITY (as CaCO3)	SILICA, SiO2	CHLORIDE, Cl	SULPHATE, SO4	NITRATE, NO3	BICARBONATE, HCO3	CARBONATE, CO3	FLUORIDE, F	NaCl, (calc from chloride)
8145358	26/06/1998	6.5	689	389	7	3	73	39	0.1	342	383	21	2	12	1	467	0	0.2	3
8145358	19/11/1998	7.3	687	394	5	2	85	38	< 0.1	368	388	19	10	16	2	473	0	0.3	16
8145358	25/03/1999	7.1	700	376	5	2	82	37	0.5	357	370	24	8	13	2	451	0	0.3	13
8145358	29/07/1999	7.0	689	387	5	2	84	37	< 0.1	362	379	20	7	16	2	462	0	0.3	12
8145358	07/09/1999	7.1	687	399	7	2	90	39	< 0.1	385	375	19	9	13	1	457	0	0.2	15
8145358	21/10/1999	7.1	690	366	5	2	88	40	< 0.1	384	376	20	9	14	2	459	0	0.3	15
8145358	24/11/1999	7.5	690	388	6	2	81	39	< 0.1	363	376	20	8	18	2	458	0	0.2	13
8145358	25/01/2000	7.1	692	389	5	2	86	39	0.1	375	375	22	8	17	2	457	0	0.2	13
8145358	04/04/2000	7.1	688	369	5	2	86	39	0.1	375	367	19	8	12	2	447	0	0.3	13
8145358	29/05/2000	7.4	692	368	6	2	83	38	0.1	363	379	20	10	15	2	462	0	0.3	16
8145358	21/06/2000	7.1	678	369	5	2	84	39	0.1	370	373	24	8	18	2	455	0	0.2	13
8145358	11/08/2000	7.6	679	387	5	2	81	38	0.1	358	380	20	8	17	2	463	0	0.3	13
8145358	08/09/2000	7.4	674	379	5	2	85	39	0.1	372	376	20	9	19	2	459	0	0.3	15
8145358	17/10/2000	7.4	681	377	6	2	85	38	0.1	368	375	25	8	16	2	457	0	0.2	13
8145358	24/11/2000	7.6	711	359	5	2	82	37	0.1	357	358	27	9	16	2	437	0	0.2	15
8145358	26/04/2001	6.9	689	370	6	2	82	36	3.6	353	370	20	11	14	3	451	0	0.3	18

## Springvale Spring G8140317

SPRING REGISTERED NUMBER	DATE OF SAMPLING	pH	ELECTRICAL CONDUCTIVITY ( $\mu$ S at 25° C) Field/Lab	TOTAL DISSOLVED SOLIDS (mg/l by evaporation at 180° C)	SODIUM, Na	POTASSIUM, K	CALCIUM, Ca	MAGNESIUM, Mg	IRON (TOTAL), Fe	TOTAL HARDNESS (as CaCO <sub>3</sub> )	TOTAL ALKALINITY (as CaCO <sub>3</sub> )	SILICA, SiO <sub>2</sub>	CHLORIDE, Cl	SULPHATE, SO <sub>4</sub>	NITRATE, NO <sub>3</sub>	BICARBONATE, HCO <sub>3</sub>	CARBONATE, CO <sub>3</sub>	FLUORIDE, F	NaCl, (calc from chloride)
8140317	20/12/1974	7.7	610	350	10	5	76	33	0.5	325	315		10	16		384		0.3	16
8140317	31/07/1975	7.8	630	360	9	6	73	30	0.4	306	308		8	22		376		0.3	13
8140317	18/03/1998	7.3	705	391	12	4	76	40	0.1	354	368	15	17	28	2	449	0	0.3	28
8140317	13/05/1998	6.6	730	416	11	4	73	41	0.1	351	388	23	7	21	2	473	0	0.3	12
8140317	21/05/1998	6.5	731	419	12	4	69	42	0.1	345	388	23	5	20	2	473	0	0.3	8
8140317	19/11/1998	7.2	750	435	12	4	86	42	0.1	387	388	21	17	25	3	473	0	0.4	28
8140317	25/03/1999	7.2	735	396	14	4	78	40	0.1	359	374	24	18	22	2	456	0	0.4	30
8140317	29/07/1999	7.1	744	423	12	3	83	42	< 0.1	380	393	22	14	23	3	479	0	0.4	23
8140317	07/09/1999	7.1	746	437	13	4	88	43	< 0.1	396	391	21	15	19	3	477	0	0.4	25
8140317	21/10/1999	7.0	749	401	12	3	88	45	< 0.1	405	390	22	16	22	3	476	0	0.4	26
8140317	24/11/1999	7.6	752	422	12	4	82	43	< 0.1	382	394	22	16	25	2	480	0	0.4	26
8140317	25/01/2000	7.2	748	433	13	4	84	43	< 0.1	386	390	28	17	27	3	476	0	0.4	28
8140317	04/04/2000	7.1	690	374	12	4	76	39	0.1	350	350	23	14	18	2	427	0	0.4	23
8140317	29/05/2000	7.5	723	405	12	4	77	41	0.1	361	378	24	18	24	2	461	0	0.4	30
8140317	21/06/2000	7.2	722	398	12	4	81	42	0.1	375	380	28	14	26	2	463	0	0.4	23
8140317	11/08/2000	7.6	731	416	12	4	82	43	0.1	381	389	18	14	27	2	474	0	0.4	23
8140317	08/09/2000	7.4	734	414	12	4	85	43	0.1	389	388	24	15	30	3	473	0	0.4	25
8140317	17/10/2000	7.3	733	405	11	4	84	43	0.1	386	386	26	14	25	3	471	0	0.3	23
8140317	24/11/2000	7.5	771	395	12	4	81	41	< 0.1	371	390	32	6	26	3	475	0	0.4	10
8140317	26/04/2001	6.8	701	386	12	4	75	38	3.8	343	359	8	16	22	2	438	0	0.4	26

# CSIRO (Hot Spring) G8140312

SPRING REGISTERED NUMBER	DATE OF SAMPLING	pH	ELECTRICAL CONDUCTIVITY ( $\mu$ S at 25° C) Field/Lab	TOTAL DISSOLVED SOLIDS (mg/l by evaporation at 180° C)	SODIUM, Na	POTASSIUM, K	CALCIUM, Ca	MAGNESIUM, Mg	IRON (TOTAL), Fe	TOTAL HARDNESS (as CaCO3)	TOTAL ALKALINITY (as CaCO3)	SILICA, SiO2	CHLORIDE, Cl	SULPHATE, SO4	NITRATE, NO3	BICARBONATE, HCO3	CARBONATE, CO3	FLUORIDE, F	NaCl, (calc from chloride)
8140312	01/12/1963	7.0	660							350	390		20						33
8140312	20/12/1963	7.7	443							370	390		15						25
8140312	02/07/1968	7.0	630	357	5	3	85	35	0.1	356	360		10	5		220		0.2	16
8140312	10/09/1975	7.3	760	380	5	4	91	39	0.1	388	381		7	14		465		0.2	12
8140312	26/09/1986		707																
8140312	18/05/1998	6.3	686	401	5	3	76	38	0.1	346	390	26	3	12	< 1	476	0	0.2	5
8140312	19/11/1998	7.3	691	395	5	3	88	39	0.1	380	385	25	7	16	< 1	470	0	0.3	12
8140312	29/07/1999	7.1	697	399	5	3	84	39	< 0.1	370	393	26	4	15	< 1	479	0	0.3	7
8140312	07/09/1999	7.1	698	409	6	3	89	41	< 0.1	391	390	25	5	14	< 1	476	0	0.3	8
8140312	21/10/1999	7.2	700	380	5	3	88	42	< 0.1	392	392	26	6	14	< 1	478	0	0.2	10
8140312	24/11/1999	7.4	703	399	5	3	83	40	< 0.1	372	393	26	3	18	< 1	479	0	0.2	5
8140312	25/01/2000	7.1	693	413	5	3	86	41	< 0.1	383	393	28	4	18	< 1	479	0	0.2	7
8140312	04/04/2000	7.1	679	377	5	3	86	40	< 0.1	379	384	26	5	17	< 1	468	0	0.3	8
8140312	29/05/2000	7.4	700	386	5	3	82	40	< 0.1	369	395	26	6	16	< 1	481	0	0.3	10
8140312	21/06/2000	7.2	692	378	5	3	85	40	< 0.1	377	391	32	4	17	< 1	477	0	0.2	7
8140312	11/08/2000	7.4	681	390	5	3	85	40	< 0.1	377	394	27	4	18	< 1	480	0	0.3	7
8140312	08/09/2000	7.3	694	396	5	3	87	42	< 0.1	390	393	27	7	20	< 1	479	0	0.3	12
8140312	17/10/2000	7.3	689	382	5	3	86	40	0.1	379	393	31	5	16	1	479	0	0.2	8
8140312	24/11/2000	7.7	723	359	5	3	78	39	< 0.1	355	394	35	4	12	< 1	480	0	0.2	7
8140312	26/04/2001	6.8	701	386	12	4	75	38	3.8	343	359	8	16	22	2	438	0	0.4	26



## **Appendix B**

### **Morphometry of Karst Depressions**

## Measurements made to estimate the geometry of karst depressions

L <sub>1</sub> and L <sub>2</sub> longest and shortest part respectively of the depression long axis on each side of the lowest point													
W <sub>1</sub> and W <sub>2</sub> longest and shortest part respectively of the depression width axis on each side of the lowest point, measured at right angles to the axis													
W <sub>max</sub> maximum width axis measured at right angles to the long axis but not necessarily passing through the lowest point													
No	AMG easting	AMG northing	Shortes part (L2) of Long axis m	Longest part (L1) of Long axis m	Long axis (L1+L2) m	Orientation degree	Shortes part (W2) of Short axis m	Longest part (W1) of Short axis m	Short axis (W1+W2) m	Shote axis (Wmax) m	Depth of depression m	Ratio length/width (L1+L2)/(Wmax)	Comments
1	221380	8390220	20	600	620	144	30	50	80	340	0.9	1.82	
2	221500	8389920	30	80	110	160	30	30	60	60	0.9	1.83	
3	221310	8389650	30	30	60	156	30	40	70	70	0.1	0.86	
4	221980	8389810	40	270	310	100	20	80	100	110	0.9	2.82	
5	222450	8389750	50	50	100	168	30	40	70	80	1.1	1.25	
6	222610	8388500	130	130	260	48	80	90	170	170	2.1	1.53	holding water in April 1998
7	223290	8388870	20	30	50	89	20	20	40	40	0.2	1.25	
8	224120	8388980	20	40	60	60	10	20	30	30	0.5	2.00	
9	221870	8387670	20	180	200	4	20	70	90	180	1.5	1.11	holding water in April 1998
10	222540	8387060	40	160	200	138	40	40	80	120	1	1.67	
11	222500	8388668	60	90	150	168	30	50	80	100	1.8	1.50	
12	223650	8387640	30	40	70	126	20	20	40	40	0.4	1.75	holding water in April 1998
13	224240	8387310	70	110	180	12	60	80	140	160	1.2	1.13	holding water in April 1998
14	224550	8387580	30	60	90	178	20	30	50	50	1.3	1.80	
15	224770	8387190	30	130	160	120	30	40	70	70	0.4	2.29	
16	225480	8387700	30	30	60	2	30	30	60	60	0.6	1.00	
17	226170	8386750	40	60	100	176	20	30	50	50	0.9	2.00	
18	226280	8386300	20	150	170	10	10	10	20	220	2.7	0.77	
19	226430	8386150	60	80	140	172	20	60	80	190	1.9	0.74	
20	225250	8386110	50	230	280	102	20	100	120	200	2.3	1.40	
21	227240	8386500	20	820	850	112	20	90	110	540	4.8	1.57	
22	228440	8386280	20	40	60	106	20	20	40	40	0.8	1.50	
23	227160	8384730	50	90	140	152	40	40	80	80	1	1.75	
24	226950	8384820	50	50	100	46	30	40	70	70	0.8	1.43	
25	226690	8385070	20	30	50	130	20	20	40	40	0.7	1.25	
26	227190	8385430	20	30	50	136	20	20	40	40	0.4	1.25	
27	226660	8385920	40	60	100	80	40	40	80	80	0.7	1.25	
28	225650	8385970	90	110	200	56	30	70	100	100	1.7	2.00	
29	225940	8383870	50	200	250	50	70	150	220	250	1.4	1.00	
30	221500	8384830	80	120	200	152	30	50	80	90	0.3	2.22	
31	221940	8383380	50	160	210	160	60	100	160	160	1	1.31	holding water in April 1998
32	221380	8381650	30	40	70	126	30	30	60	60	1.5	1.17	holding water in April 1998

## Measurements made to estimate the geometry of karst depressions

No	AMG easting	AMG northing	Shortes part (L2) of Long axis	Longest part (L1) of Long axis	Long axis (L1+L2)	Orientation	Shortes part (W2) of Short axis	Longest part (W1) of Short axis	Short axis (W1+W2)	Shote axis (Wmax)	Depth of depression	Ratio length/width (L1+L2)/(Wmax)	Comments
			m	m	m	degree	m	m	m	m	m		
33	221100	8381630	20	40	60	156	10	40	50	60	0.5	1.00	
34	212150	8389610	50	100	150	142	40	30	70	70	1	2.14	
35	212340	8389820	20	120	140	170	20	40	60	80	0.3	1.75	
36	212620	8389790	80	130	210	62	40	60	100	100	1	2.10	
37	213070	8390200	30	50	80	44	20	40	60	60	0.7	1.33	
38	213740	8389720	30	40	70	84	20	30	50	50	1.2	1.40	
39	214040	8389310	50	60	110	160	20	30	50	70	1.8	1.57	
40	214050	8389020	30	50	80	62	20	30	50	50	4	1.60	
41	214500	8389050	50	370	420	138	50	130	180	180	1.9	2.33	
42	214400	8388870	20	40	60	108	10	10	20	20	0.5	3.00	
43	215190	8388680	40	200	240	48	20	40	60	100	2.6	2.40	
44	215470	8388670	20	90	110	34	20	30	50	50	0.9	2.20	
45	215560	8389120	70	120	190	110	50	100	150	150	1.5	1.27	
46	215900	8389280	20	80	100	154	20	50	70	70	0.4	1.43	
47	215410	8389460	30	270	300	49	30	190	220	220	0.9	1.36	
48	216420	8389430	100	220	320	92	40	100	140	150	2.4	2.13	holding water in April 1998
49	216500	8389660	60	90	150	12	20	120	140	140	2.6	1.07	
50	216590	8389380	30	170	200	140	30	70	100	100	2	2.00	holding water in April 1998
51	216660	8389460	40	40	80	140	10	30	40	40	0.6	2.00	
52	216770	8389770	70	110	180	18	50	80	130	130	2.1	1.38	holding water in April 1998
53	217210	8389770	40	140	180	44	40	60	100	120	1	1.50	holding water in April 1998
54	217160	8389110	20	150	170	6	30	50	80	150	0.9	1.13	holding water in April 1998
55	216670	8388860	20	140	160	24	20	50	70	100	0.3	1.60	holding water in April 1998
56	216340	8388910	50	100	150	118	40	50	90	100	0.5	1.50	holding water in April 1998
57	216180	8388810	60	80	140	96	30	90	120	120	0.7	1.17	holding water in April 1998
58	216500	8390440	80	90	170	130	70	70	140	140	1.2	1.21	holding water in April 1998
59	217450	8388330	80	150	230	2	100	110	210	210	1.8	1.10	holding water in April 1998
60	216950	8388060	110	290	400	0	80	80	160	160	0.6	2.50	holding water in April 1998
61	216240	8388270	20	140	160	76	30	30	60	180	0.3	0.89	
62	216240	8387890	140	260	400	112	50	200	250	270	1.7	1.48	holding water in April 1998
63	216740	8387320	40	70	110	84	20	30	50	60	0.1	1.83	holding water in April 1998
64	216470	8387140	60	80	140	80	50	60	110	110	1.2	1.27	
65	216360	8386280	40	160	200	36	40	90	130	170	1.5	1.18	holding water in April 1998
66	216000	8386900	40	180	220	18	20	40	60	60	1.4	3.67	holding water in April 1998
67	217010	8386100	250	320	570	176	170	300	470	470	2.9	1.21	holding water in April 1998

## Measurements made to estimate the geometry of karst depressions

No	AMG easting	AMG northing	Shortes part (L2) of Long axis	Longest part (L1) of Long axis	Long axis (L1+L2)	Orientation	Shortes part (W2) of Short axis	Longest part (W1) of Short axis	Short axis (W1+W2)	Shote axis (Wmax)	Depth of depression	Ratio length/width (L1+L2)/(Wmax)	Comments
			m	m	m	degree	m	m	m	m	m		
68	217570	8386610	130	210	340	122	160	160	320	340	2.7	1.00	holding water in April 1998
69	217200	8386740	40	60	100	74	40	40	80	80	1.1	1.25	holding water in April 1998
70	217900	8388960	30	160	190	12	20	30	50	90	1.2	2.11	holding water in April 1998
71	218310	8390780	50	90	140	178	40	70	110	110	0.2	1.27	holding water in April 1998
72	218420	8390600	20	80	100	26	30	30	60	60	0.1	1.67	holding water in April 1998
73	218120	8388120	20	40	60	124	20	20	40	40	0.6	1.50	
74	219300	8388620	40	60	100	160	30	30	60	60	0.2	1.67	holding water in April 1998
75	218840	8387550	10	40	50	172	10	30	40	40	0.2	1.25	
76	218390	8387200	30	110	140	38	30	90	120	140	2.4	1.00	holding water in April 1998
77	218640	8387440	40	40	80	108	10	40	50	50	0.3	1.60	
78	218830	8387110	30	50	80	146	20	40	60	60	1.2	1.33	
79	218600	8386910	10	80	90	74	10	30	40	40	1.4	2.25	
80	218820	8386080	20	30	50	130	10	30	40	40	0.3	1.25	holding water in April 1998
81	219290	8386270	10	200	210	160	10	40	50	60	1.1	3.50	holding water in April 1998
82	219400	8389620	20	50	70	60	20	20	40	40	1.1	1.75	
83	220200	8386090	60	80	140	56	10	20	30	50	0.9	2.80	
84	219910	8386630	40	310	350	118	80	90	170	170	1.7	2.06	
85	223800	8386620	30	30	60	162	10	10	20	20	0.2	3.00	
86	219740	8386910	90	90	180	74	50	50	100	100	0.9	1.80	
87	219530	8386840	10	90	100	168	10	40	50	70	1.3	1.43	
88	220570	8387130	40	60	100	43	10	10	20	30	2	3.33	
89	220080	8387540	10	120	130	62	30	50	80	110	1.1	1.18	
90	219700	8387600	10	110	120	44	10	40	50	50	0.2	2.40	
91	220580	8388220	40	110	150	148	40	40	80	80	1.5	1.88	
92	220630	8388440	10	90	100	46	20	40	60	60	0.2	1.67	
93	220680	8388940	50	120	170	44	20	70	90	120	0.6	1.42	
94	220450	8389670	20	50	70	132	10	40	50	50	0.1	1.40	
95	220930	8389690	50	60	110	172	40	60	100	100	1	1.10	
96	220880	8389000	60	70	130	90	30	40	70	70	0.1	1.86	
97	219080	8385880	20	100	120	48	20	40	60	80	1.2	1.50	holding water in April 1998
98	219420	8385340	20	90	110	164	10	50	60	60	1.5	1.83	
99	220130	8385280	10	50	60	158	10	40	50	50	0.9	1.20	
100	220360	8385380	20	80	100	172	10	50	60	60	1	1.67	
101	218920	8385120	20	30	50	50	10	30	40	40	0.4	1.25	
102	219750	8395010	30	220	250	16	60	70	130	260	3	0.96	

## Measurements made to estimate the geometry of karst depressions

No	AMG easting	AMG northing	Shortes part (L2) of Long axis	Longest part (L1) of Long axis	Long axis (L1+L2)	Orientation	Shortes part (W2) of Short axis	Longest part (W1) of Short axis	Short axis (W1+W2)	Shote axis (Wmax)	Depth of depression	Ratio length/width (L1+L2)/(Wmax)	Comments
			m	m	m	degree	m	m	m	m	m		
103	217800	8384500	40	60	100	150	40	50	90	100	1	1.00	
104	218470	8384680	130	130	260	158	70	100	170	170	3.2	1.53	
105	220470	8384280	50	310	360	72	30	140	170	170	1.9	2.12	
106	215040	8383380	30	500	530	116	30	140	170	340	3.2	1.56	holding water in April 1998
107	216020	8383160	20	80	100	0	10	40	50	50	0.7	2.00	holding water in April 1998
108	216710	8383000	60	110	170	176	70	80	150	150	1.5	1.13	holding water in April 1998
109	219630	8383460	20	20	40	22	10	20	30	30	1	1.33	
110	219610	8383320	20	30	50	168	10	10	20	20	0.4	2.50	
111	216590	8383620	140	140	280	118	80	100	180	200	1.9	1.40	
112	219860	8382900	60	140	200	164	30	130	160	160	2.8	1.25	
113	220300	8382580	10	90	100	10	10	50	60	60	1.2	1.67	
114	220970	8381980	30	80	110	80	20	20	40	40	0.3	2.75	
115	215820	8381120	10	70	80	114	20	20	40	40	1.6	2.00	
116	217240	8398310	40	220	260	348	40	110	150	190	1.3	1.37	
117	212180	8398220	30	50	80	106	20	40	60	60	3.9	1.33	
118	218580	8399410	20	40	60	108	20	20	40	40	0.6	1.50	
119	219430	8399250	30	160	190	158	20	30	50	160	1	1.19	
120	220780	8399670	30	60	90	40	20	30	50	70	1.4	1.29	
121	220230	8396820	70	110	180	166	30	100	130	130	1.3	1.38	
122	219810	8396310	70	210	280	90	40	40	80	120	0.6	2.33	
123	220210	8396330	10	60	70	2	10	40	50	50	0.3	1.40	
124	220710	8395680	40	40	80	158	30	30	60	60	0.4	1.33	
125	212870	8395420	40	60	100	166	10	30	40	40	0.5	2.50	
126	214130	8396640	10	70	80	138	10	40	50	50	0.1	1.60	
127	215600	8396830	10	30	40	150	10	20	30	30	1	1.33	
128	212780	8393400	50	190	240	178	50	50	100	100	0.1	2.40	holding water in April 1998
129	216320	8393390	30	40	70	180	20	40	60	60	0.5	1.17	holding water in April 1998
130	217370	8393040	40	80	120	170	20	20	40	60	1.2	2.00	
131	212380	8392550	40	60	100	128	10	40	50	50	0.1	2.00	
132	212450	8392210	160	260	420	126	80	130	210	210	0.3	2.00	
133	213480	8392150	20	30	50	116	20	20	40	40	0.1	1.25	holding water in April 1998
134	213840	8392420	30	60	90	152	20	40	60	60	0.2	1.50	holding water in April 1998
135	214230	8392940	30	50	80	116	40	40	80	80	0.8	1.00	holding water in April 1998
136	214320	8392180	70	100	170	52	20	30	50	50	0.4	3.40	holding water in April 1998
137	215950	8392400	20	50	70	90	20	20	40	50	0.2	1.40	holding water in April 1998

## Measurements made to estimate the geometry of karst depressions

No	AMG easting	AMG northing	Shortes part (L2) of Long axis	Longest part (L1) of Long axis	Long axis (L1+L2)	Orientation	Shortes part (W2) of Short axis	Longest part (W1) of Short axis	Short axis (W1+W2)	Shote axis (Wmax)	Depth of depression	Ratio length/width (L1+L2)/(Wmax)	Comments
			m	m	m	degree	m	m	m	m	m		
138	216340	8392200	10	70	80	172	20	20	40	50	0.2	1.60	holding water in April 1998
139	216690	8392250	60	100	160	36	50	90	140	140	0.8	1.14	holding water in April 1998
140	216780	8392010	100	300	400	160	90	150	240	240	0.8	1.67	holding water in April 1998
141	228250	8397070	60	100	160	166	70	70	140	140	0.4	1.14	
142	229150	8397200	80	80	160	146	60	60	120	120	0.3	1.33	
143	225100	8395420	30	160	190	82	10	90	100	100	2.1	1.90	
144	221280	8396930	50	50	100	142	30	40	70	70	1.5	1.43	
145	228990	8392850	20	320	340	68	50	50	100	350	3.2	0.97	
146	208820	8402470	40	130	170	18	20	30	50	50	0.4	3.40	
147	208650	8402980	30	50	80	86	20	20	40	40	0.4	2.00	
148	206400	8403170	40	120	160	32	30	60	90	90	1.6	1.78	
149	205980	8403050	100	260	360	120	20	50	70	70	1	5.14	
150	205230	8402970	10	40	50	138	10	10	20	20	2	2.50	
151	205320	8402740	30	120	150	178	30	40	70	70	0.1	2.14	
152	204960	8402960	40	60	100	102	20	30	50	50	0.4	2.00	
153	205570	8403810	80	130	210	152	10	70	80	80	1.1	2.63	
154	206300	8401530	30	80	110	140	20	30	50	50	0.4	2.20	
155	204080	8401480	20	150	170	120	30	60	90	90	1.5	1.89	
156	203730	8401700	20	60	80	86	20	20	40	40	1.4	2.00	
157	203650	8401700	20	30	50	112	20	20	40	40	1.5	1.25	
158	204212	8402023	10	30	40	80	10	20	30	30	8	1.33	
159	203670	8401110	20	30	50	140	20	20	40	40	0.1	1.25	
160	204220	8400840	20	30	50	108	10	10	20	20	1.3	2.50	
161	204580	8400440	40	60	100	18	10	10	20	30	0.5	3.33	
162	204800	8400200	50	90	140	172	20	50	70	70	0.5	2.00	
163	203750	8399890	20	30	50	16	10	20	30	30	1.4	1.67	
164	203790	8400120	20	120	140	10	10	10	20	20	0.2	7.00	
165	203450	8398590	50	60	110	166	30	40	70	70	0.8	1.57	
166	203820	8399090	30	50	80	74	20	40	60	60	0.6	1.33	
167	203650	8398760	30	40	70	38	10	20	30	30	2.2	2.33	
168	203200	8399120	40	60	100	88	20	20	40	40	0.2	2.50	
169	205040	8398510	10	20	30	160	10	10	20	20	0.2	1.50	
170	204980	8398470	30	40	70	26	10	10	20	20	0.2	3.50	
171	204820	8398430	30	40	70	178	5	5	10	10	0.9	7.00	
172	205450	8398280	60	140	200	166	30	50	80	80	1.3	2.50	

## Measurements made to estimate the geometry of karst depressions

No	AMG easting	AMG northing	Shortes part (L2) of Long axis m	Longest part (L1) of Long axis m	Long axis (L1+L2) m	Orientation degree	Shortes part (W2) of Short axis m	Longest part (W1) of Short axis m	Short axis (W1+W2) m	Shote axis (Wmax) m	Depth of depression m	Ratio length/width (L1+L2)/(Wmax)	Comments
173	205830	8398230	20	30	50	140	20	20	40	40	0.3	1.25	
174	206160	8398620	20	50	70	150	10	40	50	50	0.4	1.40	
175	207430	8398170	30	60	90	112	20	40	60	60	0.6	1.50	
176	207470	8398780	20	40	60	120	10	40	50	50	0.3	1.20	
177	207760	8398570	70	100	170	78	60	60	120	120	0.3	1.42	
178	207880	8398440	70	100	170	20	20	100	120	120	0.5	1.42	
179	207700	8398320	30	60	90	130	20	30	50	70	0.4	1.29	
180	208530	8398370	15	60	75	170	10	20	30	30	0.4	2.50	
181	209140	8398820	20	20	40	139	10	20	30	30	0.5	1.33	
182	209830	8398140	30	140	170	34	25	30	55	60	1.3	2.83	
183	210650	8389530	25	45	70	20	20	40	60	80	0.8	0.88	
184	210450	8399650	10	30	40	102	5	25	30	30	0.4	1.33	
185	205900	8399260	30	60	90	68	20	20	40	40	0.9	2.25	
186	207210	8399090	30	60	90	66	10	20	30	30	0.7	3.00	
187	206130	8399570	15	20	35	30	10	20	30	30	0.3	1.17	
188	206210	8399400	20	40	60	150	10	10	20	20	0.6	3.00	
189	205170	8396500	1320	1300	2620	69	580	900	1480	1480	1.6	1.77	
190	205450	8397320	100	80	180	172	20	60	80	80	1.2	2.25	
191	203330	8396240	30	150	180	48	20	110	130	130	0.6	1.38	
192	207885	8397350	20	20	40	90	10	10	20	20	0.2	2.00	
193	208880	8395420	40	50	90	152	10	50	60	60	1	1.50	
194	209280	8395540	20	40	60	120	10	10	20	20	0.2	3.00	
195	210640	8396650	50	60	110	126	30	30	60	30	0.8	3.67	
196	211450	8396930	30	50	80	174	20	50	70	70	0.2	1.14	
197	210970	8396020	20	40	60	86	10	20	30	30	0.8	2.00	
198	211880	8395650	40	80	120	156	50	60	110	110	0.8	1.09	
199	210120	8394380	50	100	150	160	10	50	60	60	0.2	2.50	
200	210480	8393580	70	120	190	14	70	70	140	80	1.4	2.38	
201	209860	8393400	20	60	80	76	20	20	40	40	1.2	2.00	
202	196300	8406930	50	90	140	90	20	30	50	50	1.7	2.80	
203	196330	8406490	30	50	80	92	20	30	50	50	2.5	1.60	
204	196460	8406350	20	20	40	100	10	10	20	20	0.3	2.00	
205	194100	8405550	30	110	140	1	30	50	80	100	1	1.40	
206	194090	8405250	100	110	210	158	50	70	120	120	1.9	1.75	
207	195730	8405850	40	100	140	176	30	60	90	90	1.9	1.56	

## Measurements made to estimate the geometry of karst depressions

No	AMG easting	AMG northing	Shortes part (L2) of Long axis m	Longest part (L1) of Long axis m	Long axis (L1+L2) m	Orientation degree	Shortes part (W2) of Short axis m	Longest part (W1) of Short axis m	Short axis (W1+W2) m	Shote axis (Wmax) m	Depth of depression m	Ratio length/width (L1+L2)/(Wmax)	Comments
208	197640	8405230	80	100	180	100	10	50	60	60	1.5	3.00	
209	198300	8405470	50	80	130	132	20	80	100	100	3	1.30	
210	190680	8405160	70	100	170	124	40	50	90	90	1.3	1.89	
211	199040	8405920	70	90	160	88	30	40	70	80	1.2	2.00	
212	199770	8405740	30	70	100	160	20	30	50	50	0.8	2.00	
213	195160	8404740	30	100	130	162	40	60	100	100	2	1.30	
214	197000	8404460	20	20	40	20	10	10	20	20	0.7	2.00	
215	197830	8404900	30	30	60	24	20	20	40	40	0.5	1.50	
216	198670	8404440	70	90	160	142	40	60	100	100	0.5	1.60	holding water in April 1998
217	200650	8404140	90	100	190	6	30	50	80	80	0.9	2.38	
218	194560	8403080	10	30	40	54	10	10	20	20	0.2	2.00	
219	197280	8403960	20	80	100	110	20	40	60	60	1.2	1.67	
220	197480	8403560	30	90	120	140	10	30	40	100	0.7	1.20	
221	199040	8403450	40	80	120	76	20	30	50	50	1.5	2.40	
222	200940	8403950	10	10	20	46	4	5	9	9	1.7	2.22	
223	196450	8402850	40	180	220	28	70	100	170	210	1.2	1.05	
224	196360	8402910	10	30	40	23	5	10	15	15	0.7	2.67	
225	196240	8402230	20	90	110	48	30	50	80	80	1.8	1.38	
226	197060	8401970	30	50	80	148	30	30	60	60	1	1.33	
227	200790	8402370	30	70	100	120	20	30	50	50	1.7	2.00	
228	200990	8402700	10	30	40	8	10	10	20	20	0.6	2.00	
229	196870	8401560	70	120	190	1	60	100	160	165	1.9	1.15	
230	197060	8401680	30	40	70	125	20	30	50	50	0.2	1.40	
231	196960	8401170	20	70	90	126	30	30	60	60	2.4	1.50	
232	202360	8401180	50	60	110	158	20	30	50	50	1.5	2.20	
233	197420	8400780	60	310	370	154	90	150	240	240	2.6	1.54	
234	199520	8399830	20	30	50	116	10	15	25	25	0.2	2.00	
235	199270	8400230	30	270	300	96	20	80	100	200	0.5	1.50	
236	200680	8398680	10	90	100	150	20	40	60	60	1	1.67	
237	200280	8399700	20	25	45	60	10	20	30	30	0.6	1.50	
238	200460	8399710	10	30	40	70	10	20	30	30	0.3	1.33	
239	200720	8399420	90	100	190	104	40	100	140	140	1.8	1.36	
240	200770	8398840	80	100	180	170	50	90	140	140	0.3	1.29	
241	201120	8399150	20	25	45	2	10	20	30	30	0.5	1.50	
242	201360	8398720	50	60	110	158	20	50	70	70	1	1.57	

## Measurements made to estimate the geometry of karst depressions

No	AMG easting	AMG northing	Shortes part (L2) of Long axis	Longest part (L1) of Long axis	Long axis (L1+L2)	Orientation	Shortes part (W2) of Short axis	Longest part (W1) of Short axis	Short axis (W1+W2)	Shote axis (Wmax)	Depth of depression	Ratio length/width (L1+L2)/(Wmax)	Comments
			m	m	m	degree	m	m	m	m	m		
243	201320	8398520	10	60	70	172	10	20	30	70	1	1.00	
244	201410	8398390	20	50	70	172	10	30	40	40	1	1.75	
245	201240	8399270	30	40	70	116	20	30	50	50	0.1	1.40	
246	201520	8399370	20	50	70	150	10	10	20	40	0.3	1.75	
247	201710	8399650	10	60	70	82	15	20	35	35	1	2.00	
248	201390	8399690	20	25	45	172	15	25	40	40	0.9	1.13	
249	201410	8399860	25	40	65	128	10	15	25	25	0.7	2.60	
250	201600	8400140	30	170	200	70	20	45	65	65	2	3.08	
251	201950	8400190	50	60	110	128	20	25	45	45	0.5	2.44	
252	202060	8400400	40	70	110	156	30	30	60	60	0.2	1.83	
253	202220	8400040	20	50	70	176	10	30	40	40	0.4	1.75	
254	202620	8400260	20	30	50	144	10	20	30	30	0.2	1.67	
255	201770	8400800	10	30	40	132	10	20	30	30	0.5	1.33	
256	189820	8409820	20	180	200	128	30	40	70	90	1.8	2.22	
257	189190	8409330	20	40	60	156	10	30	40	50	0.5	1.20	
258	189820	8409020	20	30	50	168	20	20	40	40	0.4	1.25	
259	191520	8407940	30	190	220	132	30	70	100	100	2.1	2.20	
260	192580	8408340	20	25	45	170	5	10	15	15	0.2	3.00	
261	191930	8408770	20	30	50	106	10	30	40	40	0.9	1.25	
262	191930	8408540	10	20	30	160	10	10	20	20	0.4	1.50	
263	193290	8408040	80	240	320	126	60	80	140	140	1.7	2.29	
264	193890	8407990	50	60	110	18	20	50	70	100	0.9	1.10	
265	191500	8407560	20	50	70	144	10	35	45	45	0.5	1.56	
266	190820	8407550	20	100	120	54	20	30	50	50	3.6	2.40	
267	192040	8407120	40	45	85	26	20	30	50	50	0.3	1.70	
268	191180	8407070	50	140	190	136	20	90	110	140	0.4	1.36	
269	191510	8406120	40	60	100	152	20	30	50	60	0.5	1.67	
270	192090	8405780	30	50	80	112	20	50	70	70	1.7	1.14	
271	192280	8405830	30	160	190	4	20	90	110	140	2.6	1.36	
272	191200	8405190	10	30	40	2	15	15	30	30	1	1.33	
273	191990	8405180	30	50	80	2	10	20	30	30	0.8	2.67	
274	191520	8404800	20	240	260	126	20	140	160	180	2	1.44	
275	193590	8405310	10	50	60	8	20	30	50	50	0.9	1.20	
276	193740	8405320	70	80	150	136	10	70	80	80	1.5	1.88	
277	192830	8404900	30	120	150	166	20	50	70	70	1	2.14	

## Measurements made to estimate the geometry of karst depressions

No	AMG easting	AMG northing	Shortes part (L2) of Long axis	Longest part (L1) of Long axis	Long axis ( L1+L2)	Orientation	Shortes part (W2) of Short axis	Longest part (W1) of Short axis	Short axis (W1+W2)	Shote axis (Wmax)	Depth of depresion	Ratio length/width (L1+L2)/ (Wmax)	Comments
			m	m	m	degree	m	m	m	m	m		
278	192930	8404740	10	60	70	15	20	30	50	60	0.7	1.17	
279	191340	8404250	45	55	100	82	30	40	70	70	0.7	1.43	
280	191710	8403910	50	120	170	72	20	50	70	70	1.5	2.43	
281	192020	8403800	30	40	70	92	20	30	50	50	0.1	1.40	
282	193130	8402730	110	130	240	62	20	25	45	45	0.3	5.33	
283	200750	8397700	120	170	290	170	50	60	110	110	0.6	2.64	